AD-A058 516 AIR FORCE INST OF TECH WRIGHT-PATTERSON AFB OHIO SCH--ETC F/G 17/7
AN INVESTIGATION INTO THE VULNERABILITY OF A TYPICAL IDENTIFICA--ETC(U)
JUN 78 G S DOUPLE

UNCLASSIFIED AFIT/GE/EE/78-13 NL

1 OF 2
AD
A058516

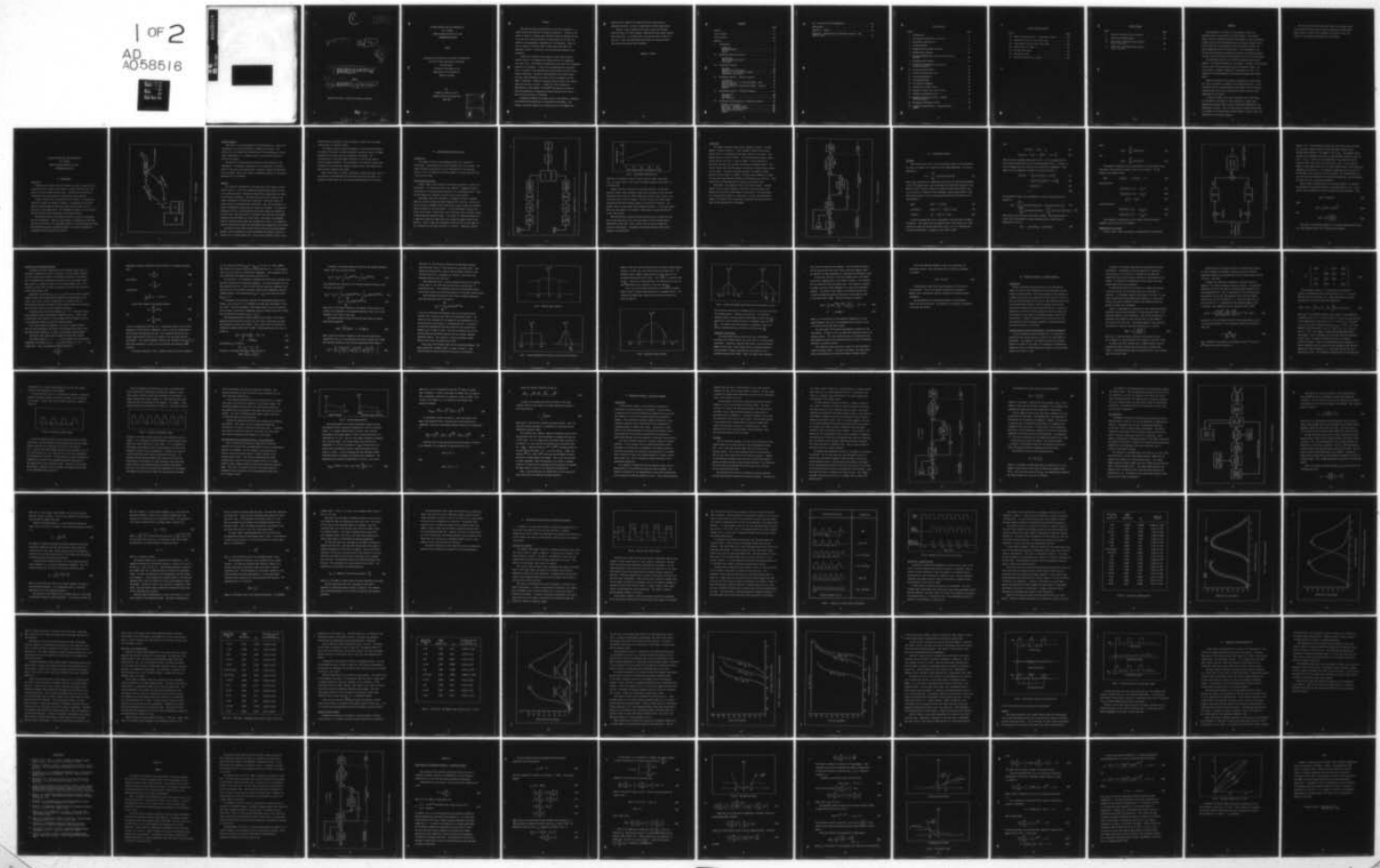

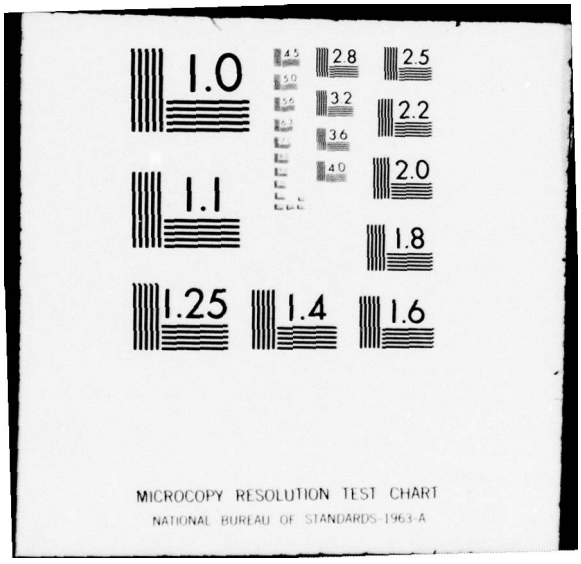
1.0
1.1
1.25
1.4
1.6
1.8
2.0
2.2
2.5
2.8
3.2
3.6
4.0
MICROCOPY RESOLUTION TEST CHART
NATIONAL BUREAU OF STANDARDS-1963-A

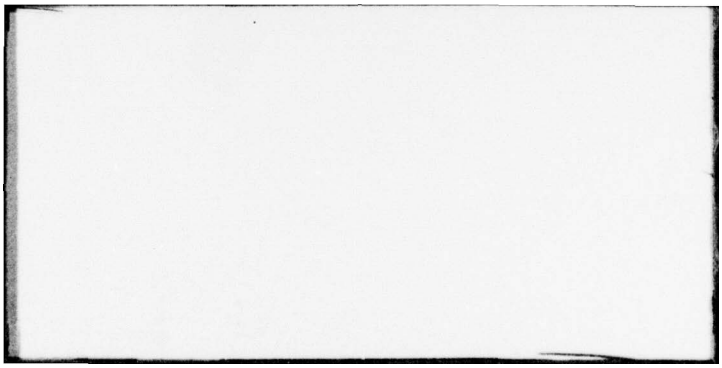

(1)

LEVEL II

(11) Jun 78

(12) 98p

DDC
RECEIVED
SEP 12 1978
F

(6) AN INVESTIGATION INTO THE VULNERABILITY OF A TYPICAL IDENTIFICATION FRIEND OR FOE (IFF) INTERROGATOR RECEIVER

(9) master's THESIS,

(14) AFIT/GE/EE/78-13

(10) Gregory S. Douple

Approved for public release; distribution unlimited

78 08 04 058

012 225

AN INVESTIGATION INTO THE VULNERABILITY OF A TYPICAL IDENTIFICATION FRIEND OR FOE (IFF) INTERROGATOR RECEIVER

THESIS

Presented to the Faculty of the School of Engineering
of the Air Force Institute of Technology
Air University
in Partial Fulfillment of the
Requirements for the Degree of
Master of Science

by

Gregory S. Douple, B.S.A.E.
Graduate Electrical Engineering

June 1978

ACCESSION for
NTIS White Section
DDC Buff Section
UNANNOUNCED
JUSTIFICATION
BY
DISTRIBUTION/AVAILABILITY CODES
Dist. SPECIAL
A

Preface

"How does one apply textbook theory to real-life problems?" is a common lament among students of graduate engineering. I undertook this project in hopes of bridging that seemingly distant gap between the two. It was my goal to apply the theory of communication to the real-life problem of electromagnetic compatability of IFF equipment. Above all else, I wanted to provide my thesis sponsor with some useful and meaningful results. To that end, this work has been personally very gratifying.

I would like to thank Mr. Don Hartman of the Flight Essential Avionics Branch in the Aeronautical Systems Division for suggesting this topic to me. His guidance and knowledge in the area of IFF equipments proved to be invaluable. I would like to acknowledge the assistance of Mr. Al Carney, of the Simulation and Testing Branch of the Air Force Avionics Laboratory. He spent a great amount of time (some of which was after hours) teaching me the use of the DEC-10 computer and the LOGIC 4 simulation. Without his expertise and assistance, this project would not have been a success. I would also like to express my appreciation to those people in the 4950th Test Wing who provided me with this opportunity to complete my graduate education full time at the Air Force Institute of Technology.

I am greatly indebted to my thesis advisor, Capt Stanley R. Robinson. He provided me with many hours of consultation and guidance. His patient, continuous support was an inspiration to me throughout this

effort, and his interest and concern for this project made its completion possible. To him, I extend my most sincere appreciation.

Finally, I wish to thank my wife, Lynn, and my two children, Britt and Jason, for their patience, understanding, and support through this trying time. I'm certain that it has been as hard on them as it was on me. Their love and devotion have made this experience much less frustrating and much more rewarding.

Gregory S. Douple

Contents

List of Figures

List of Figures (Cont'd)

List of Tables

Abstract

The performance of a typical IFF interrogator receiver was evaluated against various types of received signals. The received signals that were considered represent environments of many non-coherent friendly replies with none dominant, many non-coherent friendly replies with one dominant, noise jamming with no valid replies present, and noise jamming with one valid reply present. The performance of the receiver was determined by studying the effects of an envelope detected version of the received signal on the decoder circuit in the interrogator.

The performance analysis was initially attempted using analytic methods. This approach proved to be intractable. Therefore, the performance statistics had to be approximated using an experimental method. For this approach, a computer simulation of the decoder was used. The tightness of the approximation was evaluated by applying the Chernoff bound.

Results indicated that many types of deterministic pulse formats will cause the decoder to respond at its maximum decode rate. It was discovered that the simulated decoder would, under certain conditions, recognize pulses that did not specifically satisfy the pulse width requirement of the decoder.

In terms of random, noise-only (no dominant valid reply) types of interference, the decoder is most vulnerable to signals whose bandwidths are greater than or equal to the overall bandwidth of the interrogator receiver. Also, for these types of signals (noise-only), as the power of the interference increases beyond a certain point, the performance of the decoder improves.

For the signal-plus-noise case (one dominant valid reply present in the received signal), results indicate that once the interference power reaches a certain value, increases in the power of the valid reply will not improve the performance of the decoder.

AN INVESTIGATION INTO THE VULNERABILITY OF A TYPICAL IDENTIFICATION FRIEND OR FOE (IFF) INTERROGATOR RECEIVER

I. Introduction

Background

Identification Friend or Foe (IFF systems are used in conjunction with ground-based (and airborne) radar systems to provide identification information on aircraft detected by the radar. To obtain the identification information, IFF systems employ an ask-and-answer-type procedure.

Figure 1 shows the basic operation of an IFF system. An interrogator transmits a signal to a target of interest. A transponder on the target receives the interrogation signal and replies with an answer, which is typically a pulse-coded signal. The interrogator decodes the reply (answer) and passes identification information to the radar display.

All military aircraft and commerical civilian aircraft are equippped with IFF transponders. With this large number of transponders in the field (on the order of 10^5), there conceivably could be a sericus problem associated with the electromagnetic compatibility (EMC) of a single interrogator to transponder replies from N aircraft (N>>1).

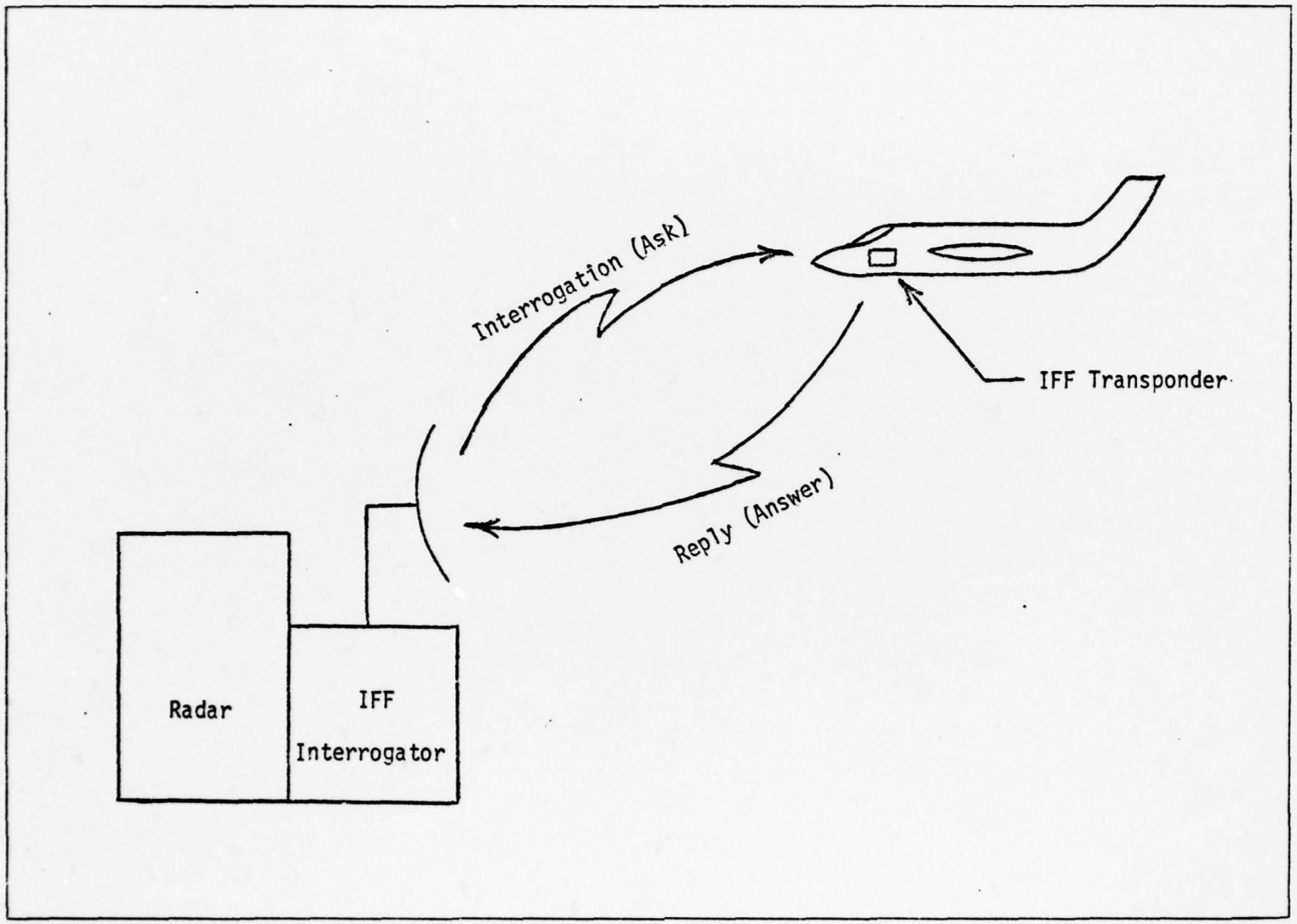

Fig 1. IFF Operation

Problem Statement

This thesis is an investigation of the vulnerability of a typical IFF interrogator to a dense environment of friendly reply signals. The analysis will also examine the vulnerability of the interrogator to intentional interference (i.e., jamming), which is of particular concern to military IFF systems.

The study will be concerned only with the receiver portion of the interrogator. No equipment nomenclature will be specified, so that the nature of the study can be generalized. No specific mode of IFF operation will be assumed. Only the two signal environments mentioned in the previous paragraph will be considered.

Approach

This study was accomplished in the three basic steps common to vulnerability analyses. First, the system being evaluated was analyzed in terms of its normal operation. Potential vulnerabilities (weaknesses) were noted as the analysis progressed. When the system analysis was completed, the signal environments of interest were identified. Statistical models for various types of interference were established. Then, the performance of a typical interrogator to these types of signals was analyzed. The measure of performance used for interference-only (noise-only) models was probability of false alarm, where false alarm is intended to mean that the interrogator interprets the interference as a valid reply. The measure of performance used for signal-plus-noise models was probability of error: the probability that the interference prevents the interrogator from recognizing a valid reply.

The results of this study indicate that a variety of fixed (non-random), periodic, pulse waveshapes will cause the modeled interrogator receiver to saturate at its maximum decode rate. Using a fixed, periodic signal, it was

discovered that the decoder in the interrogator receiver will not always reject pulses of a specified width.

For random noise-only signal environments, results show that wideband (in terms of the overall receiver bandwidth) interference results in higher probabilities of false alarm than narrowband interference. The characterisitics of the logarithmic amplifiers in the receiver tend to restrict system performance. The performance of the receiver improves when the power in the interfering signal(s) becomes greater than roughly 12 dB above minimum triggering level (MTL).

When a valid reply is present, interference signals with power levels in the region of 10 dB above MTL will effectively mask the valid reply. An increase in signal power will not improve the performance of the receiver.

II. System Description and Analysis

Introduction

This chapter presents a block diagram analysis of a typical IFF interrogator. Normal operation of the interrogator will be discussed. The signal rejection characteristics of the interrogator will be analyzed. Finally, it will be shown that the pulse decoder is the most important link in the receiver chain.

Block Diagram Description

Figure 2 shows a block diagram of the receiver portion of a typical IFF interrogator. The system consists of two, identical, independent channels. (The purpose of having two separate channels will be explained later). Since the two channels are identical, only one will be discussed here.

Transponder replies are received at a frequency of about 1 gigahertz (GHz) and filtered through the radio frequency (RF) front end. The RF front end is basically a bandpass filter that rejects signals outside the frequency range of interest to the interrogator. In the intermediate frequency (IF) strip, the RF signal is mixed with a local oscillator (LO) to produce a signal at approximately 60 megahertz (MHz). This signal is filtered and applied to a logarithmic amplifier, which serves to increase the dynamic range of the receiver. Figure 3 shows the input/output characteristics of this amplifier. It is important to note that $\log (1+X) \approx X$, for $X \ll 1$. Therefore, receiver

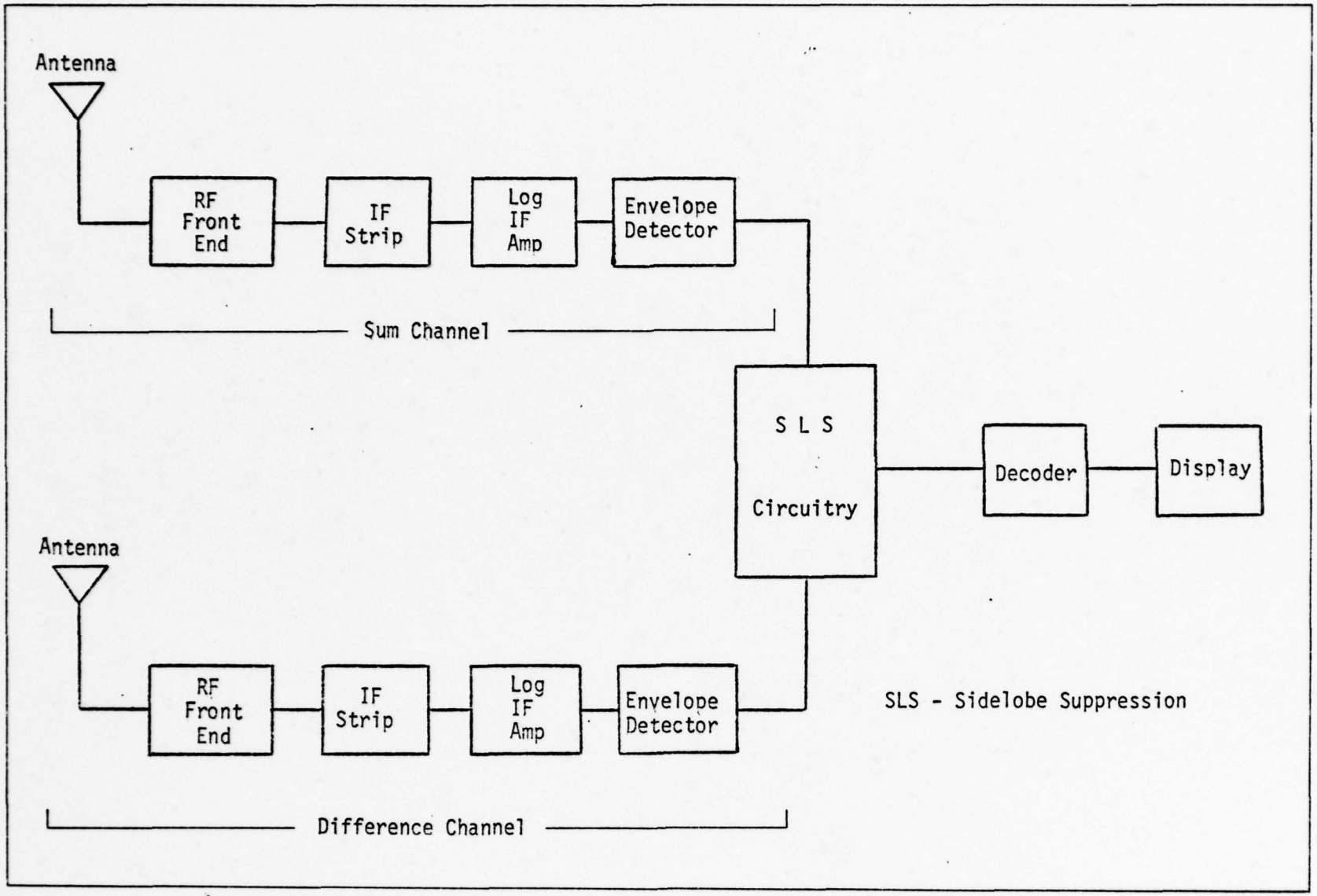

Fig 2. Interrogator Block Diagram (Receiver)

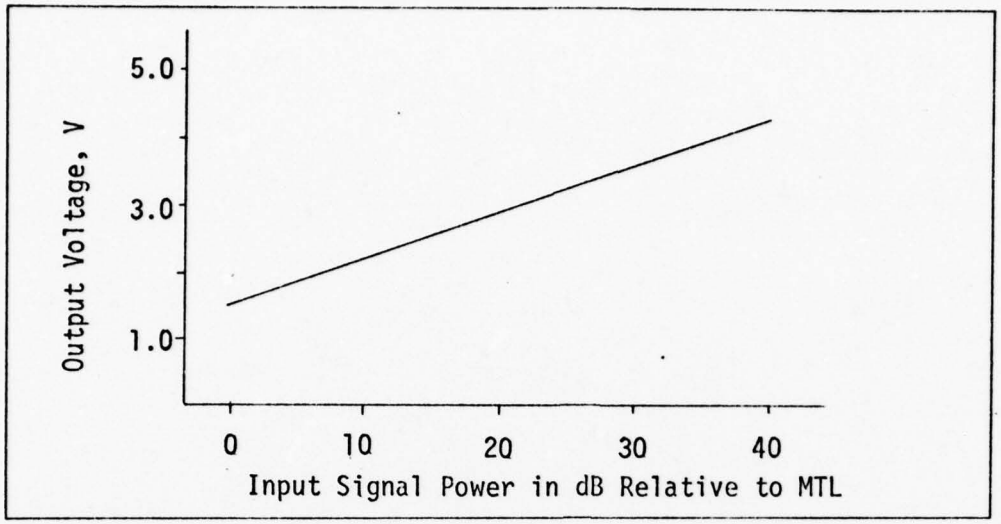

Fig 3. Input/Output Characteristic

operation is essentially linear for small values of input signal power (i.e., for power levels in the region of minimum triggering level (MTL) to 3 dB above MTL).

Signals from the IF amplifier are envelope detected. The envelope detector produces video (baseband) signals that are passed to the side lobe suppression (SLS) circuitry, which effectively discards signals that are not in the main beam of the IFF antenna. The SLS circuitry uses video signals from both the sum and difference channels to perform this function. The decoder takes the video signal and interprets the answer. If the video signal meets the requirements of the decoder, video pulses are generated and sent to the radar display.

The receiver will effectively reject signals that are outside the band-pass of the front end or not in the main beam of the IFF antenna pattern. Interference within these limits, however, will be passed through the receiver to the decoder. The decoder discriminates between valid replies (answers) and interference.

The Decoder

IFF decoders typically reply on pulse decoding circuitry. On such decoder is shown in Figure 4. It was designed to detect three pulses, each at least "α" microseconds (μsec) wide, spaced "β" μsec apart. This decoder consists of three sections. The pulse width discriminator rejects pulses that are less than "α" μsec in length. If this condition is satisfied, the pulses are applied to the pulse coincidence decoder. This circuit ensures that the three pulses are present, and that they are spaced "β" μsec apart. The pulse coincidence decoder is designed to reject pulses 3β μsec or greater in length. The pulse shaper generates a single, 0.5 μsec pulse each time the conditions of the decoder are satisfied. These video pulses are then processed for display on the radar scope.

The decoder is the important link in the receiver chain. Incoming signals on the receiver frequency (1 GHz) and in the main beam of the antenna must satisfy the requirements of the decoder if the interrogator is to interpret the signal as a valid reply. As such, the interference signals of interest to this study must be developed and characterized in terms of the requirements of the decoder.

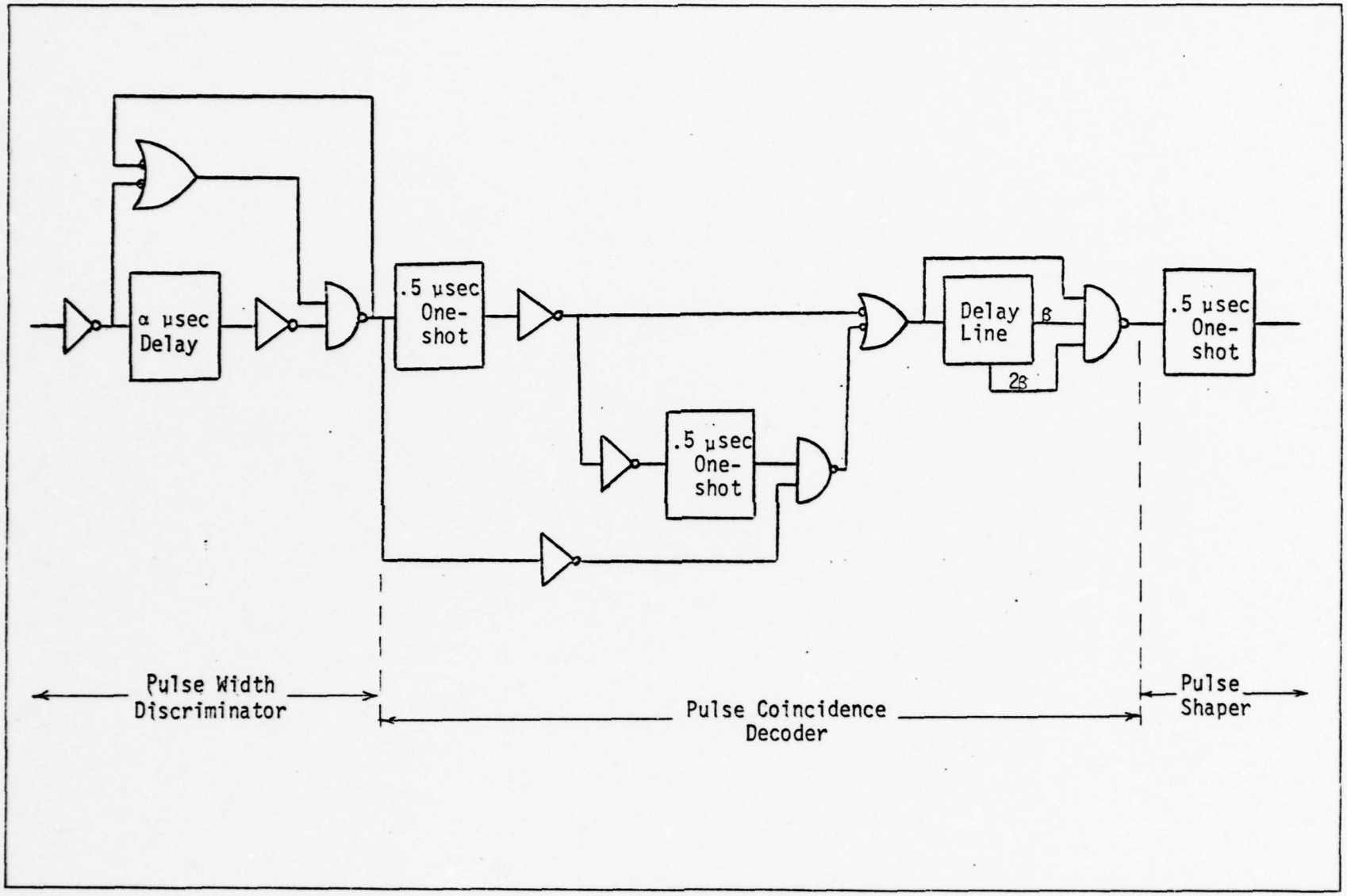

Fig 4. A Typical Decoder

III. Interference Signals

The Model

The RF signal that results from N transponder replies can be represented as a sum of N signals with random phases and random amplitudes. This can be expressed as

$$r(t) = \sum_{i=1}^{N} S_i(t)\cos\left[2\pi f_c t + \phi_i(t)\right] \tag{1}$$

where, $S_i(t)$ represents the random time variation of the amplitude (strength) of the i^{th} received signal, $\phi_i(t)$ represents the random time variation of the phase of the i^{th} received signal due to doppler and multipath effects, and f_c is the carrier frequency of the transponder replied (approximately 1 GHz). The received process, r(t), can be characterized with the following statistical moments;

mean: $$m_r(t) = E\left[r(t)\right] \tag{2}$$

correlation: $$R_r(t_1, t_2) = E\left[r(t_1)\, r(t_2)\right] \tag{3}$$

variance: $$\sigma_r^2 = R_r(t, t) - m_r(t) \tag{4}$$

It will be assumed that r(t) is stationary in the wide sense (or weakly stationary). This implies that the expected value of the process r(t), does not vary in time, and that the correlation, $R_r(t_1, t_2)$, is a function only of the time difference, τ, between t_1 and t_2 (Ref 8: 302).

Then

$$E\left[r(t)\right] = m_r(t) = m_r \tag{5}$$

$$R_r(t_1,t_2) = R_r(\tau) = E\left[r(t) \cdot r(t+\tau)\right] \tag{6}$$

Since no apriori knowledge about $\phi_i(t)$ exists, it can be assumed that the first-order distribution of $\phi_i(t)$ is uniform between 0 and 2π. Finally, it will be assumed that $S_i(t)$ and $\phi_i(t)$ are statistically independent. With these last two assumptions, the mean of the received signal is

$$E\left[r(t)\right] = E\left[S_i(t)\cos\left[2\pi f_c t + \phi_i(t)\right]\right] \tag{7}$$

$$= E\left[S_i(t)\right] E\left[\cos\left(2\pi f_c t + \phi_i(t)\right)\right] \tag{8}$$

$$= E\left[S_i(t)\right] \cdot 0 \tag{9}$$

$$= 0 \tag{10}$$

The received RF signal can be represented in terms of two quadrature components as

$$r(t) = \sum_{i=1}^{N}\left[S_i(t)\cos\phi_i(t)\cos 2\pi f_c t - S_i(t)\sin\phi_i(t)\sin 2\pi f_c t\right] \tag{11}$$

$$= \left[\sum_{i=1}^{N} S_i(t)\cos\phi_i(t)\right]\cos 2\pi f_c t - \left[\sum_{i=1}^{N} S_i(t)\sin\phi_i(t)\right]\sin 2\pi f_c t \tag{12}$$

where $S_i(t)$, $\phi_i(t)$ and f_c are as previously defined. The bracketed terms in Eq (12) can be represented as single random processes, simplifying the expression for r(t) to,

$$r(t) = n_c(t)\cos 2\pi f_c t - n_s(t)\sin 2\pi f_c t \tag{13}$$

where

$$n_c(t) = \sum_{i=1}^{N} S_i(t)\cos\phi_i(t) \tag{14}$$

and

$$n_s(t) = \sum_{i=1}^{N} S_i(t)\sin\phi_i(t) \tag{15}$$

The quadrature components can be characterized in a second-moment sense with means, autocorrelation functions, and cross-correlation. For this problem, these moments become:

mean:
$$E\left[n_c(t)\right] = E\left[n_c(t)\right] = 0 \tag{16}$$

autocorrelation:

$$E\left[n_c(t)n_s(t+\tau)\right] = R_{n_c}(\tau) \tag{17}$$

$$E\left[n_s(t)n_s(t+\tau)\right] = R_{n_s}(\tau) \tag{18}$$

$$R_{n_c}(\tau) = R_{n_s}(\tau) \tag{19}$$

cross-correlation:

$$E\left[n_c(t)n_s(t+\tau)\right] = R_{n_c n_s}(\tau) \tag{20}$$

$$E\left[n_s(t)n_c(t+\tau)\right] = R_{n_s n_c}(\tau) \tag{21}$$

The assumtion of stationarity on r(t) implies that the quadrature components $n_c(t)$ and $n_s(t)$ are stationary.

Demodulation of the Signal

Figure 5 shows a model that depicts the demodulation of the received

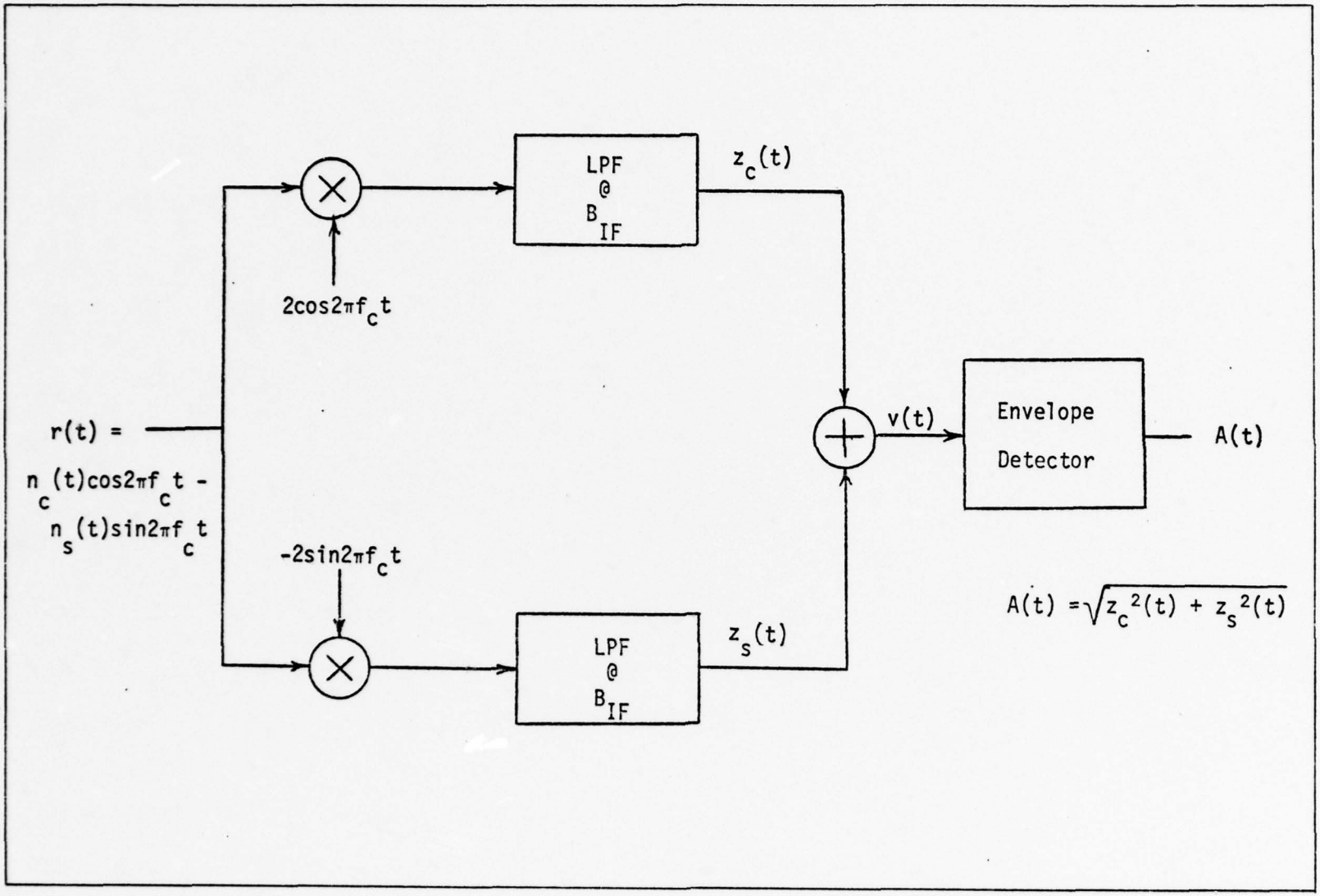

Fig 5. Demodulation of the Received Signal

process, $r(t)$. The RF quadrature signals are mixed with a local oscillator at f_c and then lowpass-filtered to block the double frequency terms. The one-sided bandwidth of the lowpass filter is B_{IF}. The baseband signals produced by the demodulation process are the quadrature components $z_c(t)$ and $z_s(t)$. If B_{IF} is greater than the bandwidths of the quadrature signals $n_c(t)$ and $n_s(t)$, then $z_c(t) = n_c(t)$ and $z_s(t) = n_s(t)$. If not, then the outputs of the lowpass filters will be band-limited versions of the quadrature components $n_c(t)$ and $n_s(t)$. The quadrature components $z_c(t)$ and $z_s(t)$ will be zero-mean, since $n_c(t)$ and $n_s(t)$ are zero-mean. The autocorrelation of $z_c(t)$ and $z_s(t)$ will depend on the relationship between B_{IF} and the bandwidths of $n_c(t)$ and $n_s(t)$, as previously mentioned.

These filtered, baseband signals are envelope detected. To emphasize the operation of the envelope detector, the baseband process $v(t) = z_c(t) + z_c(t)$ is best represented in terms of envelope and phase components. Thus,

$$v(t) = A(t)\cos\Psi(t) \tag{22}$$

where

$$A(t) = \left[z_c^{\,2}(t) + z_s^{\,2}(t) \right]^{\frac{1}{2}} \tag{23}$$

and

$$\Psi(t) = \tan^{-1}\left(\frac{z_s(t)}{z_c(t)} \right) \tag{24}$$

The output of the envelope detector is the random envelope process $A(t)$, it is this baseband signal that is applied to the decoder.

Statistics of the Detected Envelope

A complete statistical description of the envelope process, A(t), is desirable, although quite difficult to obtain. For this study, therefore, it will be sufficient to obtain a first-order description of the process. This is accomplished by determining the statistics of the random variable $A(t_1)$, which is a sample (at time t_1) of the random process, A(t). The statistics of $A(t_1)$ will be used to characterize the first-order statistics of the random process, A(t).

Henceforth, the notation n_c, n_s, z_c, z_s and A will be used to represent random variables that are obtained by sampling the random process $n_c(t)$, $n_c(t)$, $z_c(t)$, $z_s(t)$, and A(t), respectively, at a specific time, t_1. The statistics derived or assumed for these random variables will represent the first-order statistics of the respective processes.

To determine the statistical properties of A, it is necessary to make some assumptions about the quadrature components n_c and n_s. Using a form of the Central Limit Theorem, it will be shown that time samples n_c and n_s of the quadrature signals are Gaussian random variables.

Each of the quadrature components is a sum of N random variables. With very weak assumptions, the Central Limit Theorem can be used to show that these N-fold summations, n_c and n_s, are Gaussian random variables.

The Central Limit Theorem can be stated as follows (Ref 13:202):

The random variables $x_1, x_2, \ldots, x_n$ are defined to be statistacally independent, with means $m_1, m_2, \ldots, m_n$, and variances $\sigma_1^2, \sigma_2^2, \ldots \sigma_n^2$, respectively. Then, the probability density function of

$$Y \triangleq \sum_{i=1}^{n} x_i \tag{25}$$

approaches a Gaussian probability density function as n becomes large with mean

$$m = \sum_{i=1}^{n} m_i \tag{26}$$

and variance

$$\sigma^2 = \sum_{i=1}^{n} \sigma_i^2 \tag{27}$$

provided that

$$\lim_{n\to\infty} \frac{\sigma_i}{\sigma} = 0 \quad ; \quad \text{for all } i. \tag{28}$$

To apply this theorem to the random variables

$$n_c = \sum_{i=1}^{N} S_i \cos\phi_i \tag{29}$$

and

$$n_s = \sum_{i=1}^{N} S_i \sin\phi_i \tag{30}$$

it must be assumed that the terms (i.e., transponder replies) in the N-fold summations are statistically independent. Also, it must be assumed that no one individual term dominates the sum. This assumption implies that the targets (generating IFF replies) are roughly at the same range from the interrogator. This latter assumption satisfies the requirement that $\lim_{n\to\infty} \frac{\sigma_i}{\sigma} \to 0$. With these assumptions, n_c and n_s can be considered joint Gaussian random variables.

If the power spectrum of r(t) is symmetric about the carrier frequency,

f_c, the cross-correlations $R_{n_c n_s}(\tau) = R_{n_s n_c}(\tau) \equiv 0$ for all τ (Ref 13:239). This implies that $n_c(t)$ and $n_s(t)$ are uncorrelated for all t. It also implies that $n_c(t_1)$ and $n_s(t_2)$ are statistically independent. This assumption will be used to determine the probability density function for A.

At this point, it is convenient to summarize the statistical properties that have been derived for the quadrature components. With the development that has been completed thus far, it can be stated that the quadrature components $n_c(t)$ and $n_s(t)$ are (to first-order) zero-mean, statistically independent, Gaussian random processes, with autocorrelation $R_{n_c}(\tau) = R_{n_s}(\tau)$ and cross-correlation $R_{n_c n_s}(\tau) = 0$.

To determine the first-order statistics of the baseband quadrature components, $z_c(t)$ and $z_s(t)$, it is reasonable to assume that the bandpass filters are linear. With this assumption, the baseband signals are (to first-order) also zero-mean, statistically independent, Gaussian random process (Ref 13:233), with autocorrelation functions $R_{z_c}(\tau) = R_{z_s}(\tau)$.

With baseband quadrature signals defined in this manner, A will have a Rayleigh probility density function, and Ψ will have a uniform $[0, 2\pi]$ probability density function (Ref 11:427). Also, A and Ψ will be statistically independent random variables (Ref 11:366). The Rayleigh density for A can be written as

$$f_A(r) = \frac{r}{\sigma_A^2} \exp \frac{-r^2}{2\sigma_A^2} \quad ; \quad \text{for } r \geq 0 \tag{31}$$

$$= 0 \quad ; \quad \text{elsewhere.} \tag{32}$$

The quantity σ_A^2 is given by

$$\sigma_A^2 = \sigma_{z_c}^2 = \sigma_{z_s}^2 = \sigma_z^2. \tag{33}$$

The mean of a Rayleigh distributed random variable is

$$E[A] = \sqrt{\frac{\pi}{2}}\,\sigma_A = \sqrt{\frac{\pi}{2}}\,\sigma_z. \tag{34}$$

In general, the autocorrelation functions of the baseband quadrature signals $n_c(t)$ and $n_s(t)$ are given by

$$R_{n_c}(\tau) = R_{n_s}(\tau) = \int_{-\infty}^{\infty} S_{n_c}(f) e^{j2\pi f\tau} df = \int_{-\infty}^{\infty} S_{n_s}(f) e^{j2\pi f\tau} df \tag{35}$$

The autocorrelation functions of the filtered baseband processes, $z_c(t)$ and $z_s(t)$, are given by

$$R_{z_c}(\tau) = R_{z_s}(\tau) = \int_{-\infty}^{\infty} S_{n_c}(f) \left|H(f)\right|^2 e^{j2\pi f\tau} df = \int_{-\infty}^{\infty} S_{n_s}(f) \left|H(f)\right|^2 e^{j2\pi f\tau} df \tag{36}$$

$$R_{z_c}(\tau) = \int_{-B_M}^{B_M} S_{n_c}(f) \left|H(f)\right|^2 e^{j2\pi f\tau} df \tag{37}$$

where $H(f)$ is the impulse response of the lowpass filter and B_M is the minimum of the bandwidth of the baseband quadrature signal, B_n, and the bandwidth of the lowpass filter, B_{IF}.

The autocorrelation function of $A(t)$ has been shown to be (with appropriate assumption)

$$R_A(\tau) = \frac{\sigma_z^2}{2}\left[2\underline{E}(k_o) - (1 - k_o^2)\underline{K}(k_o)\right] \tag{38}$$

where $\underline{E}$ and $\underline{K}$ are elliptic integrals of the first and second kind, respectively, and k_o is the normalized correlation function (Ref 7:403). The covariance function of $A(t)$ has been approximated (Ref 6:53) as

$$C_A(\tau) = \frac{\sigma_z^2}{16}\pi\left[\left(\frac{C_z(\tau)}{\sigma_z^2}\right)^2 + \frac{1}{16}\left(\frac{C_z(\tau)}{\sigma_z^2}\right)^4 + \frac{1}{64}\left(\frac{C_z(\tau)}{\sigma_z^2}\right)^6 + \ldots\right] \tag{39}$$

where $C_z(\tau)$ is the covariance function of the baseband processes $z_c(t)$ and $z_s(t)$, and σ_z^2 is the variance of $z_c(t)$ (and $z_s(t)$). This expression indicates that a plot of the correlation function of the envelope process will, in general, be "narrower" than that of the baseband processes $z_c(t)$ and $z_s(t)$.

The correlation time, τ_c, of the envelope process will be defined as the value of τ for which the autocorrelation function $R_A(\tau)$ is approximately zero. The correlation time can be interpretted crudely as the time interval over which the process will not change "significantly".

The correlation functions for the filtered, baseband quadratures $z_c(t)$ and $z_s(t)$ were given in Eq (37) as

$$R_{z_c}(\tau) = \int_{-B_M}^{B_M} S_{n_c}(f)\left|H(f)\right|^2 e^{j2\pi f\tau} df \qquad (37)$$

It was also stated that the envelope, A(t), has an autocorrelation function that is narrower than that of the quadrature signals. The effects of this narrowing will be ignored in the determination of τ_c, since the point at which $R_A(\tau)$ is "approximately zero" is typically an arbitrary determination and hence should not vary significantly whether $R_{z_c}(\tau)$ or $R_A(\tau)$ is used. Thus, the correlation time will be derived using the correlation function for the filtered, baseband quadrature signals. This value of τ_c can be considered an upper bound on the actual correlation time of A(t).

If $B_n \geq B_{IF}$, the received signal will be considered wideband. The power spectrum of a wideband signal is shown in Figure 6. (The spectrum shown was chosen arbitrarily for ease of illustration.)

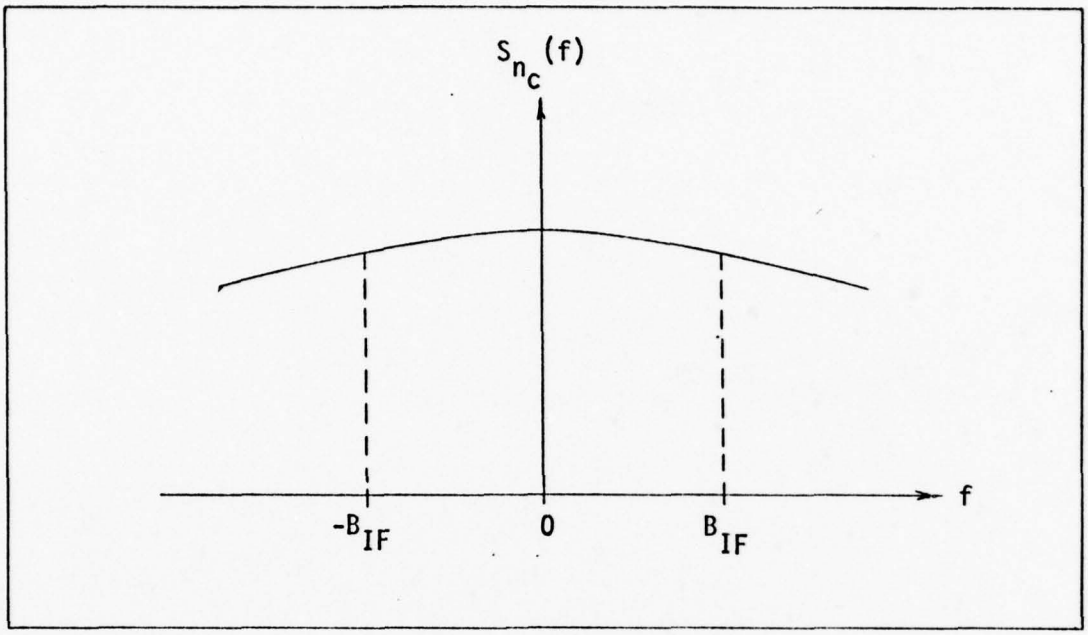

Fig 6. Wideband Power Spectrum

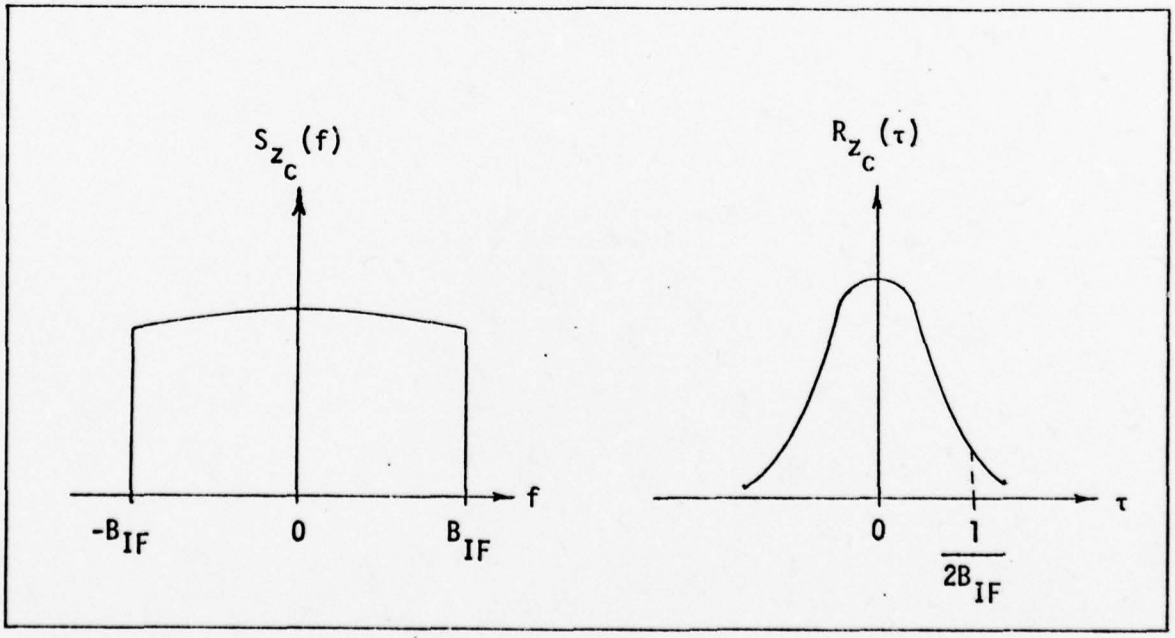

Fig 7. Filtered Wideband Power Spectrum and Correlation Function

Figure 7 shows the filtered spectrum and the resultant autocorrelation function. In this case, the filtering has been assumed ideal. For wideband signals, samples spaced greater than $\frac{1}{2B_{IF}}$ apart will be considered uncorrelated (Ref 11:403). This implies a correlation time of $\frac{1}{2B_{IF}}$. Thus, for a wideband process, the envelope signal will not vary significantly over intervals of time less than $\frac{1}{2B_{IF}}$.

If $B_n < B_{IF}$, the received signal will be considered narrowband. Figure 8 shows a typical power spectrum of a narrowband process. The filtered, narrowband power spectrum and correlation function are shown in Figure 9.

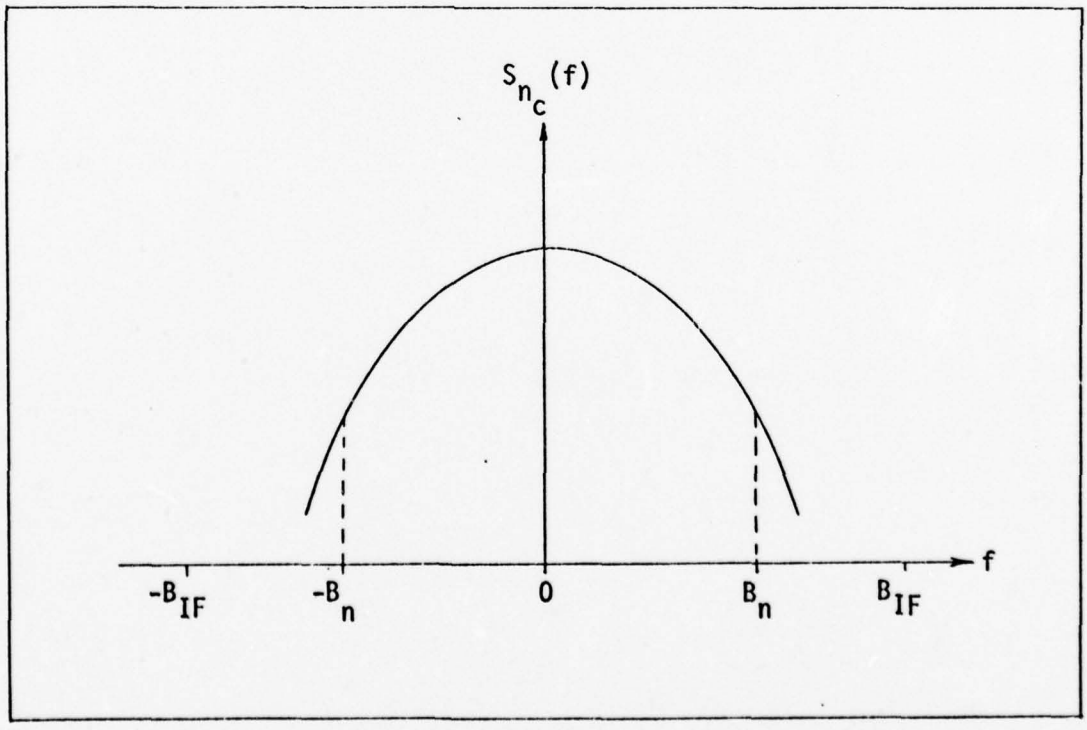

Fig 8. Narrowband Power Spectrum

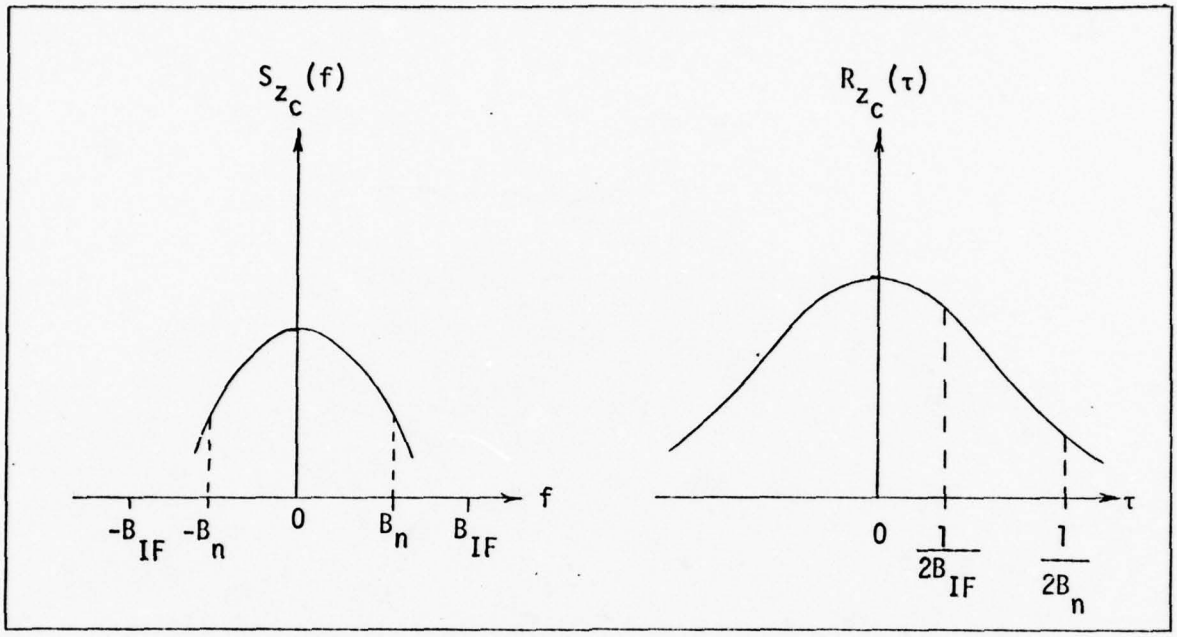

Fig 9. Filtered Narrowband Power Spectrum and Correlation Function

The correlation function for narrowband signals is less steep than that for wideband signals. Therefore, the value of τ for which two envelope samples can be considered uncorrelated is greater than $\frac{1}{2B_{IF}}$. Specifically, the correlation time for a narrowband signal will be $\frac{1}{2B_n}$. This implies that the envelope of a narrowband process will not vary significantly over intervals of time less than $\frac{1}{2B_n}$.

Intentional Interference

The signal model that has been derived for a high density environment of friendly replies also serves well for a noise jamming environment. Typically, a thermal noise source is used to modulate jammers of this type. Since thermal noise is considered Gaussian, the amplitudes of signals transmitted by noise jammers can be considered Gaussian (Ref 7:482). Thus, the signal model developed

can be used to represent noise jamming. The first-order statistics for the envelope A(t) that result from a noise-only jamming signal are identical to those developed for a high density environment signal.

Of particular interest in the noise jamming case is the effect of the noise (jamming) when a valid reply is present. This situation will be termed the signal-plus-noise case. The situation is modeled by adding a constant signal component, A, to one of the quadrature channels. The effect of this change on the envelope process A(t) is that the probability density function of a time sample of A(t) is now Rician (Ref 13:328). The Rician density is given by

$$f_A(r) = \frac{r}{\sigma_z^2} \exp\left(\frac{-(A^2 + r^2)}{2\sigma_z}\right) I_o\left[\frac{Ar}{\sigma_z^2}\right] \quad ; \quad \text{for } r \geq 0 \qquad (40)$$

$$= 0 \quad ; \quad \text{elsewhere} \qquad (41)$$

where σ_z^2 is the variance of the quadrature components, A is the signal component, and $I_o(\cdot)$ is the modified Bessel function of the first kind and zero order (Ref 13:328).

The valid reply will be within the bandwidth limitation of the interrogator. As such, it will not effect the correlation time of the envelope process. Thus, the correlation time can be determined (for both wideband processes and narrowband processes) using the technique outlined in a previous section.

The signal-plus-noise case also is useful for the high density signal environment model. In terms of that model, the signal-plus-noise case represents one strong reply among N friendly replies.

It has been mentioned (Chapter 2) that the IF amplifiers are logarithmic devices. Thus, the signal that is passed to the decoder is actually

$$L(t) = \log A(t) \tag{42}$$

A second-moment statistical characterization of L(t) proved to be intractable. This did not present a problem to the analysis, however, due to the approach that was finally used to measure system performance.

The performance of the interrogator decoder to these modeled signals can now be evaluated. The approach to the problem is presented in the next two chapters.

IV. Performance Analysis: Analytic Approach

Introduction

Having established the characteristics of the interference signals of interest, the vulnerability of the interrogator to those signals could be analyzed. The initial approach to this problem was to obtain analytically the probability of false alarm for the noise-only case and the probability of error for the signal-plus-noise case. It was established in Chapter 2 that the decoder is the primary discriminator between valid replies and interference. As such, the probability of error will be the probability that the decoder does not recognize a valid reply in an envelope-detected, signal-plus-noise process. Likewise, the probability of false alarm will be the probability that the decoder recognizes an envelope-detected, noise-only process as a valid reply.

Characterization of the Received Process: Zero Crossing Approach

In order to determine these probabilities, it is necessary to characterize the received process in terms of the requirements of the decoder. For example, if the decoder requires that incoming pulses be at least "α" μsec wide, it is necessary to determine the probability that the received process will appear to be pulses whose widths are at least "α" μsec.

In general, IFF decoders have specific pulse width and spacing requirements. The probability that the decoder will recognize a noise process as a valid reply is a function of the underlying probability that the noise process satisfies the requirements of the decoder. To establish the probability of false alarm, this underlying probability must be determined.

To characterize the pulse-like nature of a random noise process, a zero-crossing (or level-crossing) analysis of the process is necessary. If the decoder requires pulse widths of at least "α" μsec, then by analyzing the time between zero-crossings of a given noise process, one could, presumably, determine the probability that the process satisfies this requirement.

There is a great amount of information in the literature concerning zero/level crossing characterization of random processes (Ref 2 is an excellent summary of this information). Most of this information is presented in the context of zero crossing rate, N_o, the number of zero crossings per unit time. The expected number of zero crossings per second of a zero mean, Gaussian random process is given by

$$E[N_o] = \frac{1}{\pi}\left[\frac{-R_n''(0)}{R_n(0)}\right] \tag{43}$$

where $R_n(\cdot)$ is the correlation function of the process n(t) and $R_n''(\cdot)$ denotes its second derivative with respect to time (Ref 10:54).

In terms of the zero crossing rate, a wideband process could be considered one whose expected zero crossing rate is greater than 10 MHz. A narrowband process would be characterized by a zero crossing rate of less than 10 MHz.

Although the zero crossing rate serves to categorize the process as either wideband or narrowband, it does not lead to the desired underlying probability (the probability that the random process consists of pulses α μsec wide).

To obtain this underlying probability, a density function is needed for the intervals between zero/level crossings. No closed form expression exists for this density, although several approaches have been attempted (Ref 2). Most of them consist of the following steps. An expression for $p_o(\tau)d\tau$, the probability that a Gaussian random process has a zero in the interval $(\tau, \tau + d\tau)$, given that the last zero occurred at $t = 0$, regardless of what happened between 0 and τ is derived. This probability has been shown to be (Ref 2:306)

$$p_o(\tau)d\tau = \frac{1}{\pi}\left[\frac{-R_n(0)}{R_n''(0)}\right]^{\frac{1}{2}} \frac{[M_{22}^2 - M_{24}^2]^{\frac{1}{2}}}{[R_n^2(0) - R_n^2(\tau)]^{\frac{3}{2}}}\left[1 + H\tan^{-1}(H)\right] d\tau \qquad (44)$$

where $R_n(\cdot)$ is the correlation function of the random process, $R_n''(\cdot)$ is the second derivative of the correlation function with respect to time, and

$$H = \frac{M_{24}}{\left[M_{22}^2 - M_{24}^2\right]^{\frac{1}{2}}} . \qquad (45)$$

M_{ij} is defined as the cofactor of the element in the i^{th} row and the j^{th} column of the matrix M, which is

$$M = \begin{bmatrix} R_n(0) & 0 & R_n(\tau) & R_n'(\tau) \\ 0 & -R_n''(0) & -R_n'(\tau) & -R_n''(\tau) \\ R_n(\tau) & -R_n'(\tau) & R_n(0) & 0 \\ R_n'(\tau) & -R_n''(\tau) & 0 & -R_n''(0) \end{bmatrix} \tag{46}$$

This expression serves as a starting point for determining $P_o(\tau)d\tau$, the probability that a zero will occur in $(\tau, \tau + d\tau)$ given that the last zero occurred at t=0. Using the method of inclusion and exclusion, it has been shown (Ref 10:64) that

$$P_o(\tau) = p_o(\tau) - \int_0^\tau p_1(\tau_1,\tau)d\tau_1 + \frac{1}{2!}\int_0^\tau\int_0^\tau p_2(\tau_1,\tau_2,\tau)d\tau_1 d\tau_2 - \ldots \tag{47}$$

where $p_o(\tau)$ is as previously defined, $p_1(\tau_1,\tau)d\tau_1 d\tau$ is the probability of having a zero in $(\tau, \tau + d\tau)$ and in $(\tau_1, \tau_1 + d\tau_1)$; $p_2(\tau_1,\tau_2,\tau)d\tau_1 d\tau_2 d\tau$ is the probability of having zeros in $(\tau, \tau + d\tau)$, $(\tau_1, \tau_1 + d\tau_1)$ and $(\tau_2, \tau_2 + d\tau_2)$; and, in general, $p_n(\tau_n,\tau_{n-1},\tau_{n-2},\ldots,\tau)d\tau_n \ldots d\tau$ is the probability of having zeros in $(\tau_n, \tau_n + d\tau_n)$, $(\tau_{n-1}, \tau_{n-1} + d\tau_{n-1})$,..., and $(\tau, \tau + d\tau)$. The integrals in the series become progressively more complex. Also, to evaluate $P_o(\tau)$, one must study the convergence of this series. An analytic expression for $P_o(\tau)$ is extremely difficult to obtain. Even if one could obtain such an expression, it must be remembered that $P_o(\tau)$ gives only the probability that the noise process has a zero crossing in $(\tau, \tau + d\tau)$ given that the last zero crossing was at t=0. This probability alone would not be the underlying

probability that is desired (the probability that the noise process satisfies the requirements of the decoder).

To illustrate this point, it is convenient to consider an arbitrary detector, designed to detect four pulses of widths α μsec and spaced β μsec apart. A signal that satisfies these conditions is shown in Figure 10.

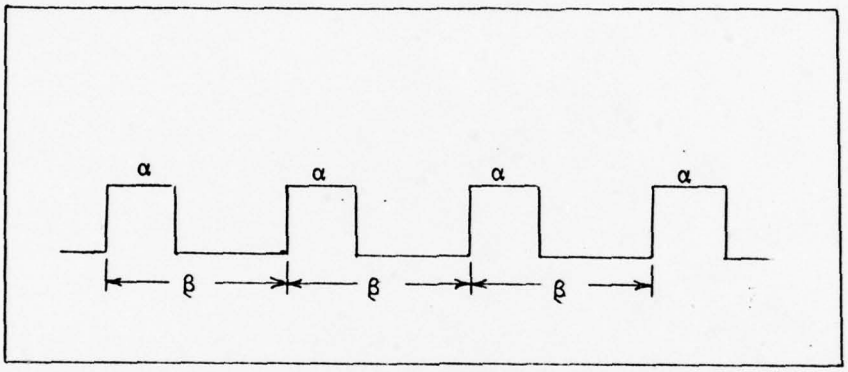

Fig 10. An Arbitrary Reply Signal

To find the probability that a noise process $x(t)$ satisfies these requirements, one must determine the joint probability that the length between successive zero crossings in $[0, \alpha]$ is in the interval $(\alpha, \alpha + d\alpha)$, and the length between successive zero crossings in $[\alpha, \beta]$ is in the interval $(\beta-\alpha, \beta-\alpha + d\beta)$, and so on, until the requirements of the decoder are specified. If these events are assumed statistically independent, the overall joint probability would be the product of the probabilities of the individual events. Logically, if $P_o(\tau)$ could be evaluated, it would be used to determine the probabilities of each of the independent events occurring.

Using the approach just outlined, one could, in principle (and with a great deal of difficulty), determine the probability that a noise process satisfies exactly the requirements of the decoder. A logical question that arises, however, is "Are these the only signal conditions that are acceptable to the decoder?" For example, a noise process could look like the signal in Figure 11. This signal consists

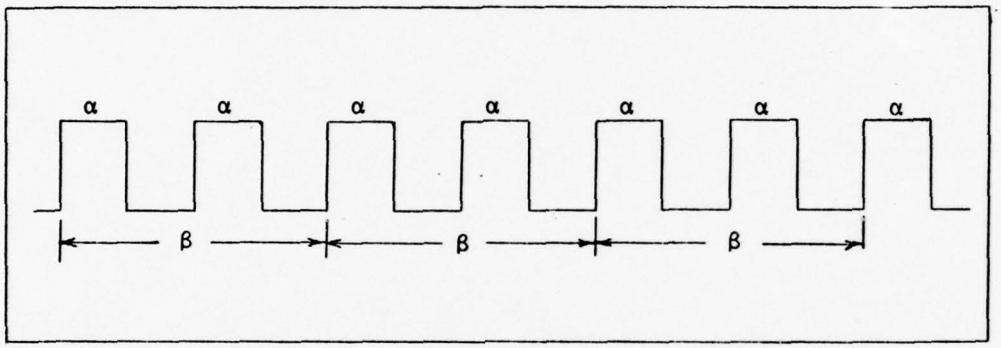

Fig 11. Arbitrary Interference Signal

of pulses α μsec wide, spaced β μsec apart, with additional pulses in between. It is important to consider whether or not the decoder would detect this sample function as a valid reply. If it is decoded as a valid reply, the probability that the noise process will take on the waveshape of Figure 11 must be determined. As before, this requires a joint probability, which could be determined using $P_o(\tau)$. To determine the underlying probability that the noise will meet the requirements of the decoder, all signal waveshapes that the process might exhibit must be evaluated against the decoder requirements. For each of the signals that satisfy the requirements of the decoder, the probability that the noise looks like that particular waveshape

must be determined, using the $P_o(\tau)$ expression as before. The underlying probability that is desired is then a function of all of these individual probabilities.

A more general approach might be to describe the sets of signals which would be correctly (or conversely, incorrectly) decoded. The underlying probability would then be an intersection (product) of the probabilities of occurrence of the signal sets that are correctly decoded. The task of identifying these signals and/or signal sets is extremely tedious and time-consuming.

The analytic approaches outlined in this section were considered unacceptable. They require the use of probability densities/distributions for which no closed form expressions exist. In addition, they require an exhaustive search for the signals (or signal sets) that could be recognized by the decoder as a valid reply.

Characterization of the Received Process: Discrete Approach

Since it proved to be analytically impossible to determine probabilities of false alarm and probabilities of error, an experimental approach was attempted. For this approach, it was necessary to develop a piece-wise constant model for sample functions of the envelope process, A(t). This involves representing the random envelope with a series of discrete, constant values, Δt in length. Figure 12 shows a sample function of x(t) and its piece-wise constant model. The value of Δt that is used for a particular model was determined by the correlation time of the quadrature signal out of the IF bandpass filter.

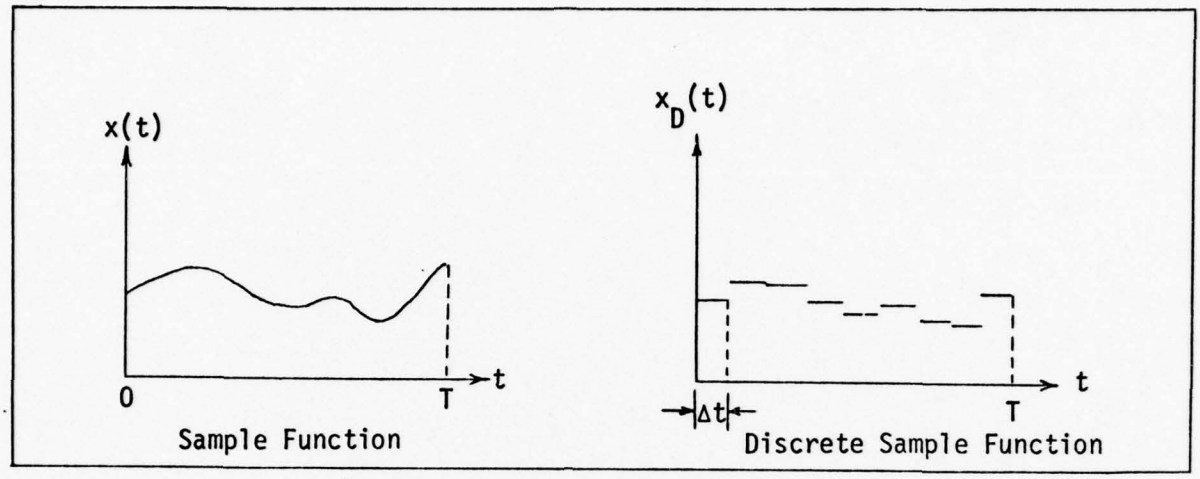

Fig 12. Discrete Approximation

The discrete model is an attractive approach, because finding the probability that a particular waveshape will exist is relatively simple. If a decoder requires pulses of width α μsec, the only requirement of the random process is that it exceed some level (i.e. threshold) for "α" μsec. This is a very simple situation to represent with a discrete model. The discrete model that satisfies this requirement is a series of N pulses, $N = \frac{\alpha}{\Delta t}$, that are equal to or greater than the threshold (level) at which the decoder sees the signal as a pulse. It will be assumed that the individual samples (discrete levels) of the model are statistically independent. The probability that a discrete random model is a pulse α μsec wide is

$$P_{x(t)=\alpha} \triangleq P[x(t) = \text{Pulse } \alpha \text{ μsec wide}] = \prod_{i=1}^{N} P[x_i \geq n] \qquad (48)$$

where $P[x_i \geq \eta]$ is the probability that the i^{th} sample is greater than a threshold, η, and N is the number of samples that are required (due to bandwidth limitations) to constitute a pulse of width α μsec. If each of the samples, x_i, are identically distributed, this probability becomes

$$P_{x(t)=\alpha} = \left(P[x_i \geq \eta]\right)^N = \left(P[x_i \geq \eta]\right)^{\frac{\alpha}{\Delta t}} \tag{49}$$

If the decoder requires two pulses, α μsec wide spaced β μsec apart, the probability that a discrete model (using statistically independent, identically distributed samples) satisfies this requirement is

$$\left(P[x_i \geq \eta]\right)^{\frac{\alpha}{\Delta t}} \cdot \left(P[x_i < \eta]\right)^{\frac{\beta-\alpha}{\Delta t}} \cdot \left(P[x_i \geq \eta]\right)^{\frac{\alpha}{\Delta t}} \tag{50}$$

Since the level of each discrete portion of the model is relative to a threshold, it is convenient to represent $P[x_i \geq \eta]$ as

$$P[x_i \geq \eta] = p \tag{51}$$

Then

$$P[x_i < \eta] = 1 - p \tag{52}$$

Using this notation simplifies Eq (50) to

$$p^{\frac{\alpha}{\Delta t}}(1-p)^{\frac{\beta-\alpha}{\Delta t}}\, p^{\frac{\alpha}{\Delta t}} = p^{\frac{2\alpha}{\Delta t}}(1-p)^{\frac{\beta-\alpha}{\Delta t}} \tag{53}$$

In terms of the probability density function of the video envelope (which has been shown to be either Rayleigh or Rician), p can be expressed as

$$p = \int_{\eta}^{\infty} f_A(\beta)\, d\beta \tag{54}$$

where $f_A(\beta)$ is the specific probability density function. Thus, for any given discrete waveshape, its probability of occurrence can be determined relatively simply.

This approach does, however, require an exhaustive search of the pulse patterns that will cause the decoder to recognize the noise as a valid reply. If it is assumed that the decoder looks for pulses in an interval of Γ μsec, and the noise process has a correlation time of $\tau = \frac{1}{2B_{IF}}$, then the effects of $2^{\Gamma/\tau} = 2^{2\Gamma B_{IF}}$ discrete versions of the noise must be analyzed. For $\Gamma = 5.0$ μsec and $B_{IF} = 5$ MHz, this involves 2^{50} (or 1.1259×10^{15}) different discrete sample functions that must be checked against the decoder. This is just for one case of signal bandwidth! When the bandwidth of the signal is changed, a new set of signals must be developed and tested against the decoder. The sheer numbers involved in this approach are prohibitive.

Thus, it was decided that the probabilities of false alarm and error would have to be determined through simulation.

V. Performance Analysis: Simulation Approach

Introduction

In the previous chapter, it was shown that evaluation of performance by analytic methods is intractable. In this chapter, an approach will be developed whereby the probability of false alarm and probability of error can be approximated using experimental methods. This experimental approach (hereafter referred to as the simulation approach) involves observation of the performance of a simulated decoder to random signal inputs. By applying a random signal to the simulated decoder and observing the resultant output, the probability of false alarm (or probability of error) can be approximated through a relative frequency of occurrence interpretation.

This type of approach requires a simulation program for decoder operation. It also requires that the random interference signals be modeled in a format that is acceptable to the decoder simulation. Once these requirements are satisfied, the performance of the decoder must be observed for many trials (applications) of a single, specific input signal case. This is necessary to obtain confidence in the approximated probability.

It is important to emphasize that this approach results only in approximations to the performance statistics that are sought. The tightness (closeness) of the approximations to the actual probabilities can be improved by conducting additional trials. Due to time constraints,

however, there was only a limited number of trials that could be conducted for each specific input signal of interest. For this study, a bound on the approximated performance statistics will be determined given a finite number of trials.

The experiments (trials) were conducted using a DEC-10 digital computer at the Air Force Avionics Laboratory (AFAL). The logic circuitry of a typical IFF interrogator decoder was simulated using the LOGIC 4 Logic Simulation & Fault Analysis program, which is described briefly in Appendix A. The LOGIC 4 program is well-suited for simulation of this type of logic circuit. The difficult aspects of this approach were adapting LOGIC 4 to accept a random input signal and monitoring its output on a continuing basis. These problems were solved using some rather unique subroutines, which were developed especially for this study.

The Model

For the simulation approach, the issue is the performance of the modeled decoder to a sample function of the random envelope signal, A(t). This is the same envelope signal that was derived in the previous chapter. All of the assumptions made for that derivation hold for the signal models used in the simulation approach. (Samples of the quadrature components were zero-mean, uncorrelated, Gaussian random variables with equal autocorrelation functions.) The statistics of A were shown to be Rayleigh for the noise-only case and Rician for the signal-plus-noise case.

The envelope process A(t) will be modeled using the piece-wise constant approximation presented in the previous chapter. The amplitude

of a single "piece" (sample) of a sample function is a random variable whose statistics are either Rayleigh or Rician. The length of the piece is a function of B_M, the minimum of the signal bandwidth and the bandwidth of the lowpass filter.

The model that was used for the decoder is shown in Figure 13. This figure is identical to Figure 4, with the exception that values have been placed on α and β from that previous figure. The circuit components were modeled as zero-delay elements (that is, the transition time between a change on the input of the element and the resultant change on the output is zero). This is a valid assumption, since all of the delays imposed on the signal by the delay lines and one-shots are greater (by at least an order of magnitude) than the nominal transition times of the other circuit elements. The one-shots in the decoder are not retriggerable, that is, once a one-shot is triggered and counting out, it can not be retriggered (have the count restarted). Thus, the outputs of the one-shots (once they have been triggered) will always be pulses of length 0.5 μsec. (This is the way that the one-shots operate in a typical decoder.)

To determine the performance statistics, the output of the decoder is observed. For the noise-only case, one observation interval is defined to be the shortest length of time over which a false alarm can be expected to occur. The one-shot on the output of the decoder limits the observation interval to 0.6 μsec, 0.5 μsec for the "on-time" of the one-shot plus 0.1 μsec for the reset time of the one-shot. Thus, the false alarm rate is limited to one every 0.6 μsec. This implies a decoded response every 0.6 μsec, or a decode rate of 1.667×10^6 decodes/second.

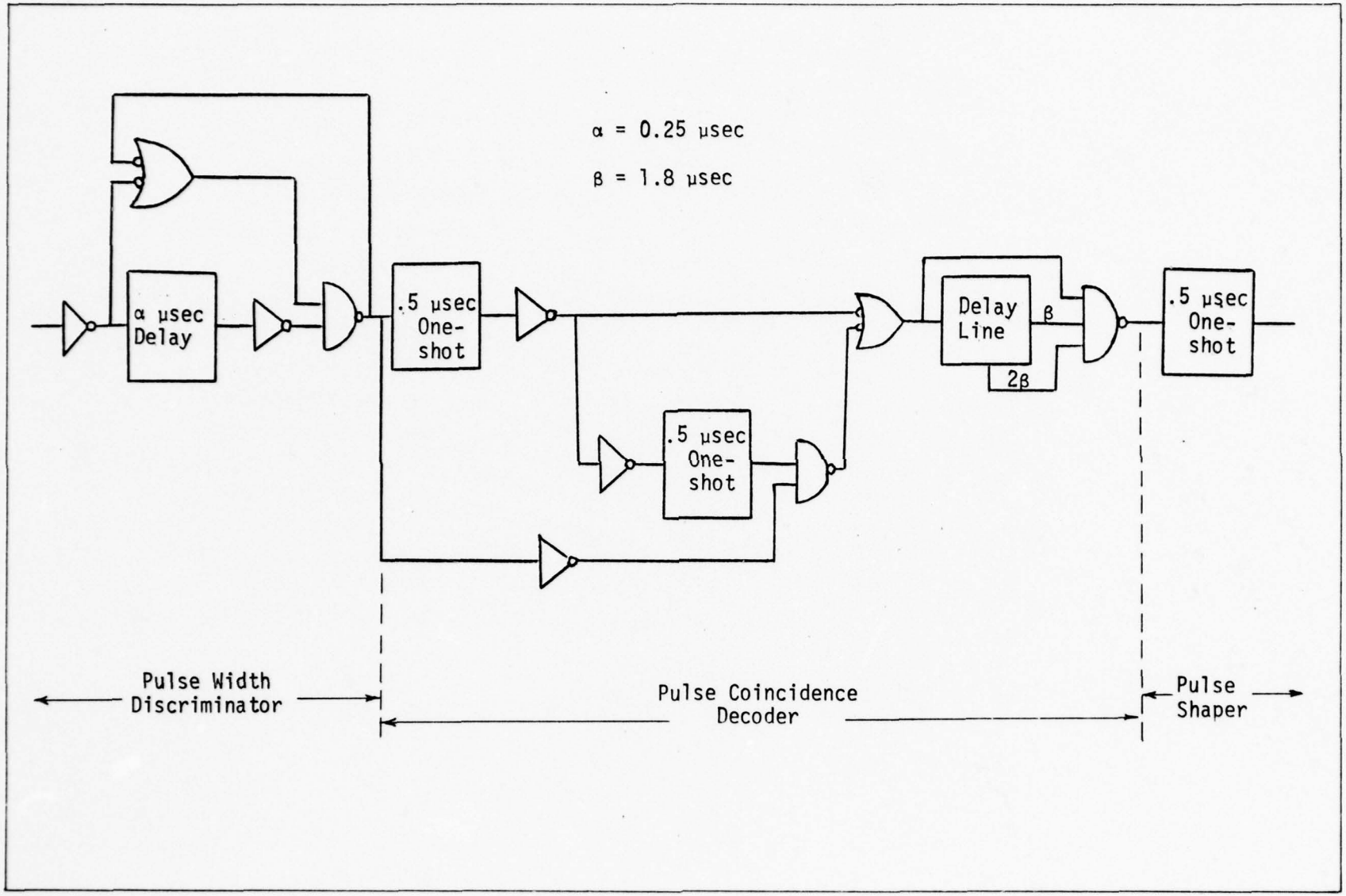

Fig 13. The Modeled Decoder

The probability of false alarm can be approximated as

$$P_{fa} \approx \frac{1}{N}\left(T_R\right) \tag{55}$$

where N is the number of observations that are made, and T_R is the number of times that the one-shot is triggered. As N increases, this approximation approaches the true probability of false alarm.

For the signal-plus-noise case, the issue is whether or not the noise masks the valid reply. To determine this, the performance of the one-shot on the output of the decoder is checked. This one-shot is observed only at the precise instant that it is expected to be triggered by the valid reply. If the one-shot is not triggered at this point, or has already been triggered, the noise has effectively masked the valid reply, and an error has been made. An observation (for this case) is defined to be the output that results from a valid reply (plus noise) input to the decoder. The interval between observations is considerably longer for the signal-plus-noise case, since time must be allowed for decoding of the valid reply.

The probability of error can be approximated by

$$P_E \approx \frac{1}{N}\left(T_E\right) \tag{56}$$

where N is the number of observations made (as before) and T_E is the number of times that the valid reply was effectively masked by the noise. Just as was the case with the P_{fa}, this approximation approaches the actual probability of error as N increases.

The tightness of the approximations can be evaluated by applying the Chernoff bound. Given an approximated probability of false alarm (or probability of error), the number of trials made, and the per cent confidence desired in the approximation, the Chernoff bound can be used to determine upper and lower bounds around the approximated probability. The Chernoff bound and its application to this study are explained in Appendix B.

The Simulation

The computer simulation can most easily be explained using the block diagram of Figure 14. All of the simulation is conducted with software. The program asks the user to specify the conditions on the input signal in terms of power and bandwidth. The LOGIC 4 simulation of the decoder circuit accepts an input every gate time, which is the basic timing unit used in this simulation. These inputs are generated in subroutines external to the LOGIC 4 simulation. The outputs of the LOGIC 4 simulation are observed and the appropriate probabilities are determined, also using a subroutine that is external to the LOGIC 4 program.

The statistics of the amplitude of each piece of the input signal are derived from a uniform random number generator (URNG) that was stored in the computer as a user-available option. This random number generator produces samples that have a probability distribution that is uniform between 0 and 1. The random number generator was seeded so that it would not start at the same point each time the simulation was run. The details of the random number generator that was used can be found in Reference 9.

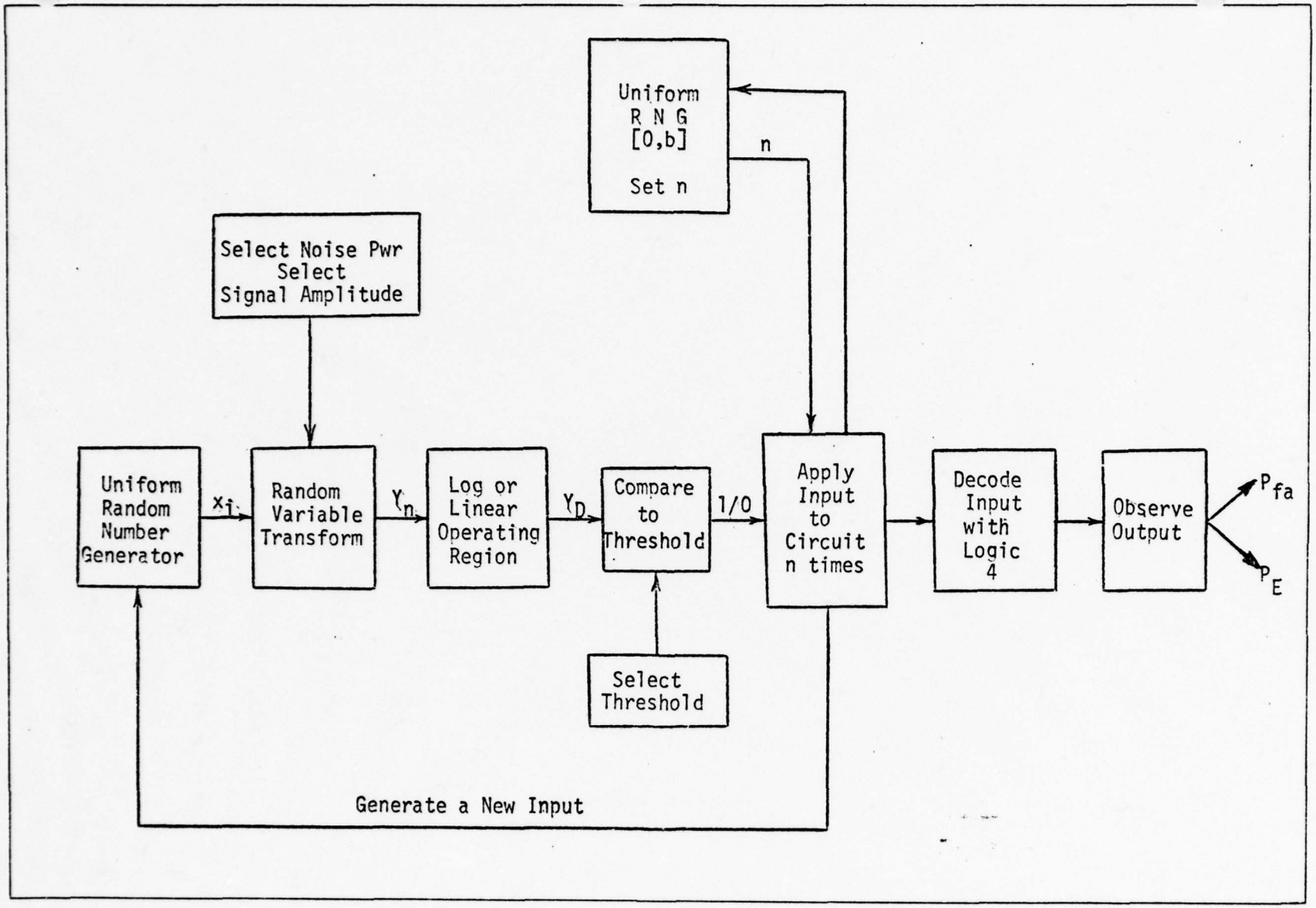

Fig 14. The Simulation Approach

The statistics of A are not uniform, so the samples derived from the URNG had to be transformed to exhibit the appropriate statistics. For the noise-only case, this was done using an algebraic transformation on the individual samples from the URNG. This transformation is given by

$$Y_i = \sqrt{-2\sigma_z^2 \ln(1 - x_i)} \tag{57}$$

where the Y_i are the Rayleigh distributed samples, the x_i are the samples from the URNG, and σ_z^2 is the variance of one of the filtered, baseband, quadrature signals (Ref 3:184-185). The square root of σ_z^2 is a measure of the root-mean-square (RMS) noise voltage of A(t).

For the signal-plus-noise case, no simple, closed-form transformation existed to obtain Rician random variables from uniform random variables. Thus, the transformation to Rician random variables was obtained by a "brute-force" technique. For this technique, Gaussian random variables were generated using samples from the URNG. For each Gaussian sample, twelve URNG samples were required. Two Gaussian samples were required (one for each quadrature component) to derive an envelope sample. Thus, 24 URNG samples were required for each envelope sample.

Each of the Gaussian quadrature samples, g_i was derived using the following expression:

$$g_i = \sigma_z \left[\left(\sum_{i=1}^{12} x_i \right) - 6.0 \right] \tag{58}$$

where the x_i's were samples from the URNG, and σ_z was the effective RMS noise voltage, as before. The "6.0" was subtracted from the sum to make the Gaussian samples zero mean.

Rayleigh distributed samples, Y_i can be obtained by taking the square root of the sum of the squares of the individual quadrature samples, i.e.,

$$Y_i = \sqrt{g_1^2 + g_2^2} \tag{59}$$

This method of generating Rayleigh distributed samples from uniformly distributed samples was used (for the noise-only cases) during the latter portion of the study. Results obtained using this method were consistent with results obtained earlier in the study, when the Rayleigh distributed samples were formed using Eq (57).

To obtain Rician random variables, it is only necessary to add a signal component, A_s, to one of the quadrature components. Thus, the envelope samples, Y_R, are forced to have Rician statistics using

$$Y_R = \sqrt{(g_1 + A_s)^2 + g_2^2} \tag{60}$$

where A_s is the value (in volts) of the signal component, and the g's are as previously defined. It is assumed here that A_s is entirely contained on one of the quadrature channels.

The samples are next identified as to whether they are in the linear or logarithmic region of receiver operation. If the value of either the

RMS noise voltage, σ_z, or the signal component, A_s, is more than 3 dB above the threshold, η (which will be discussed momentarily), the receiver will be operating in its logarithmic region. For operation in this region, the amplitude of an envelope sample is taken to be

$$Y_D = \log Y_n \tag{61}$$

where $Y_n = \sqrt{g_1^2 + g_2^2}$ for the noise-only case and $Y_n = \sqrt{(g_1 + A_s)^2 + g_2^2}$ for the signal-plus-noise case. For operation in the linear region, the amplitude of an envelope sample is simply defined as

$$Y_D = Y_n \tag{62}$$

where Y_n is defined as before.

The envelope samples Y_D are compared with a threshold, η. This comparison characterizes the envelope process as a series of 0's and 1's (0 when $Y_D < \eta$ and 1 when $Y_D \geq \eta$). The threshold physically represents the voltage level that is required before the decoder will recognize a signal. As such, the threshold can be interpretted as the MTL alluded to in Chapter 2. If the voltage of an incoming signal is less than this threshold (MTL), then that signal will not be strong enough to trigger the decoder. The actual value of this threshold is unimportant in this study. Only the relative values of RMS noise voltage and signal level to this threshold are of concern.

With the signal characterized by a series of 0's and 1's, it can now be applied to the simulated decoder. The LOGIC 4 simulation was

set up to accept a new input every gate time. Two gate times constitute one coarse time. A time scale was established that equates one coarse time to 0.1 μsec. This represents a correlation time of 0.1 μsec, which is derived from the lowpass filter bandwidth (assumed to be nominally 5 MHz). Thus, the envelope process was not allowed to vary any faster than every 0.1 μsec (i.e., every coarse time).

For those signals whose bandwidth were less than 5 MHz (with corresponding correlation times greater than 0.1 μsec), it was necessary to apply the same input (a 1 or 0) to the circuit for n coarse times, where n is determined by

$$n = \frac{\tau_s}{0.1} \tag{63}$$

and τ_s is the correlation time of the narrowband signal in μsec.

For narrowband interference, n was considered to be a random variable. This made the simulation more realistic, because it is doubtful that actual interference signals would have a constant correlation time. The distribution on n was chosen, nominally, to be uniform between 0 and some upper bound, b. As this upper bound increases (from a value of 0.1), the correlation time increases. The expected value of n is given by

$$E[n] = \frac{1}{2} b \tag{64}$$

where b is the upper limit on the uniform distribution. For wideband

signals; E[n] = 1 and τ_s = 0.1 μsec. For narrowband signals, E[n] > 1 and τ_s > 0.1 μsec.

Each gate time, the LOGIC 4 simulation accepts an input (1 or 0), even though the input can change only every coarse time. The effects of this input on the simulated decoder are computed. Then, the simulation moves on to the next gate time, asking for another input. For wideband signals, a new input is generated every coarse time. For narrowband signals, the value of the input stays constant for n coarse times (where n is determined as previously explained).

For the noise-only case, the output of the LOGIC 4 simulation is checked each gate time. Each time that the one-shot on the output is enabled (triggered), a false alarm is recorded. Since a gate time is equivalent to 0.05 μsec, and the on-time of that one-shot is 0.5 μsec, provisions were made so that each false alarm would not be counted more than once. An observation interval was defined previously to be 0.6 μsec. This corresponds to 12 gate times (6 coarse times). The probability of false alarm can be approximated by

$$P_{fa} \approx [\text{Number of False Alarms Counted}] \div \frac{N_c}{6} \qquad (65)$$

where N_c is the number of coarse times over which observations were made.

For the signal-plus-noise case, the output of the LOGIC 4 simulation is tested only when an output is expected. The rationale used to determine whether or not an error was made has been explained previously.

For each particular input signal case (noise-only or signal-plus-noise, with a specific value of RMS noise voltage, specific value of signal amplitude, and specific value of the limit on n), a great number of coarse times are required to be simulated. The Chernoff bound could be used to determine the number of trials (which implies the number of coarse times) that are needed to establish desired bounds on an approximated probability. However, since only a limited number of trials could be made, the Chernoff bound was used to determine the bounds that can be placed on an estimated probability once a given number of trials (coarse times) are simulated.

The results obtained from this simulation and the corresponding bounds that were achieved are presented in the following chapter.

VI. Presentation and Discussion of Experimental Results

In Chapter V, an experimental method of determining probabilities of false alarm and probabilities of error was described. A computer simulation was used to conduct the experiments and determine the probabilities. In this chapter, the results of that computer simulation will be presented and analyzed.

Periodic Pulse Signals

The simplest signal model tested was a repeating (periodic) pulse signal. This type of signal is shown in Figure 15. All pulses are a constant α μsec wide and spaced a constant γ μsec apart. The amplitude of each pulse was required only to be above MTL for the entire duration of the pulse. This implies that the decoder "sees" each of the pulses.

This type of signal was most useful in debugging the computer simulation. Given a fixed input signal, the output of the decoder could be easily determined (without use of the simulation). By applying the same periodic signal to the simulated decoder and observing the output, the validity of the simulation could be verified.

This type of signal model can be used to represent a periodic-pulse-type of interference. In terms of unintentional interference, this implies that transponder replies from many targets line up in time to produce a periodic pulse pattern. In terms of intentional interference, this type of signal could be used to model a fixed duty cycle (fixed pulse width and fixed pulse repetition frequency) jammer.

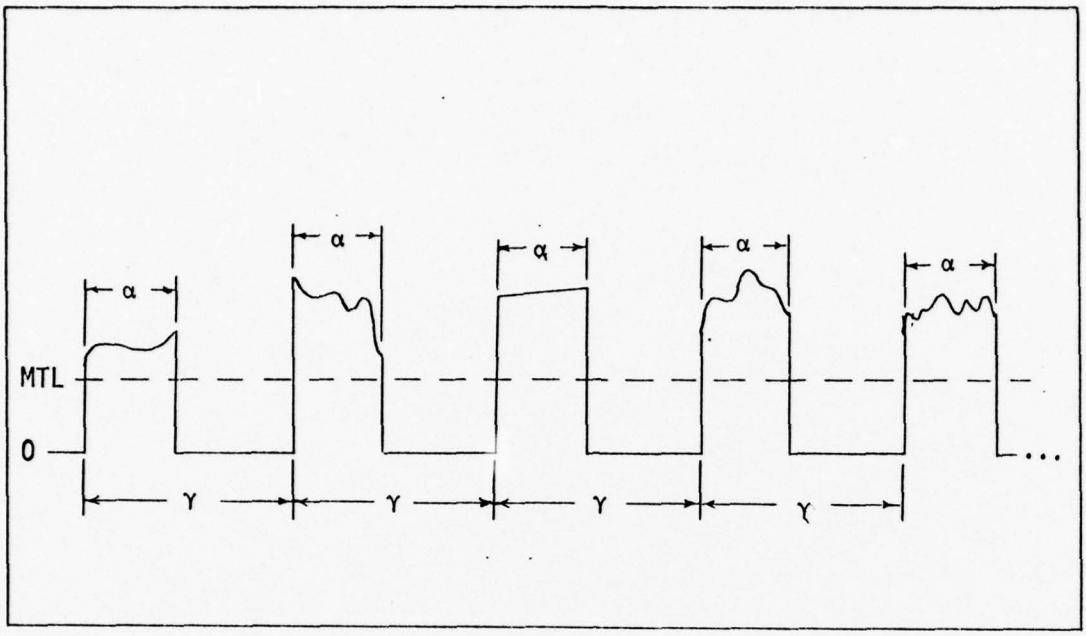

Fig 15. Periodic Pulse Signal Format

Periodic pulse signals that will have the most significant effect on the decoder are those whose values of α and γ satisfy, respectively, the pulse width and pulse spacing requirements established by the decoder. For the simulated decoder, pulses must be at least 0.25 μsec wide and 1.8 μsec apart. This decoder requires that three pulses be present with these widths and spacings. A decode is generated for each set of three pulses (triplet) that satisfies these requirements. Since periodic pulse signals (as modeled here) are not random, the measure of performance will be the number of decodes per second that result from a specific input. A single, correct, reply signal results in 300 decodes per second (nominally). This implies a nominal spacing between triplets of 3.33 msec.

It was shown in Chapter V that an observation interval was determined by the on-time and recovery-time of the one-shot on the output of the decoder.

This time interval (on-time pulse recovery time) was 0.6 μsec for the computer simulation. With the length of an observation interval set at 0.6 μsec, only one false alarm can occur in an observation interval (since the length of a decode is determined by the on-time of the one-shot on the output of the decoder). If a decode occurs every 0.6 μsec, the resultant number of decodes per second is 1.667×10^6. This is the maximum decode rate of the simulated decoder, and it is four orders of magnitude greater than the nominal decode rate (300 decodes/second).

The periodic pulse formats tested against the simulated decoder are listed in Table I, along with the corresponding decode rates that were observed. This table shows only a few of the many periodic pulse formats that could have been tested. Of primary concern are those input pulse signal formats that result in the maximum decode rate. The pulse formats of Table I that result in this maximum decode rate by no means constitute all such possible formats. It is only important to note that the maximum decode rate is realizable with a number of different periodic pulse formats.

Perhaps the most significant result shown in Table I is that the decoder will not always reject pulses of widths less than 0.25 μsec. This phenomenon is best explained with the use of the timing diagram shown in Figure 16. Signals that are less than 0.25 μsec wide and spaced less than 0.25 μsec will cause the pulse width discriminator to be enabled. Figure 16 shows that the pulse width discriminator is enabled when a pulse of width 0.1 μsec is present coincident with a previous pulse, which has been delayed 0.25 μsec. The output that is generated progresses through the decoder as if the input pulses had satisfied the pulse width requirement of the decoder.

Periodic Pulse Format*	Decode Rate
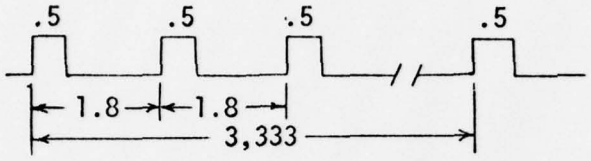	300
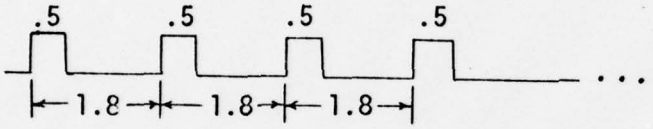	5.55×10^5
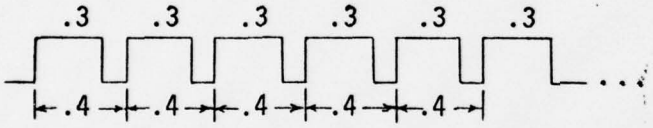	1.67×10^6 (Max)
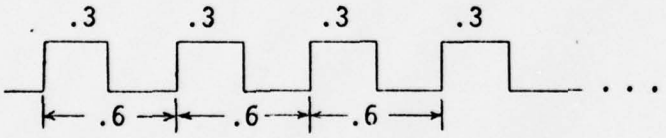	1.67×10^6 (Max)
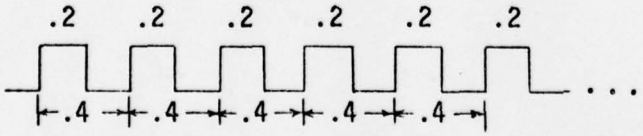	1.25×10^5
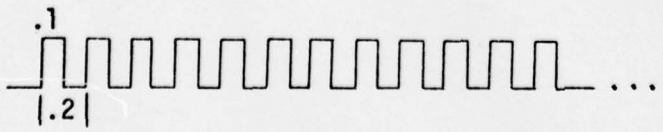	1.67×10^6 (Max)
*Pulse Parameters in μsec	

Table I. Results of Periodic Pulse Interference

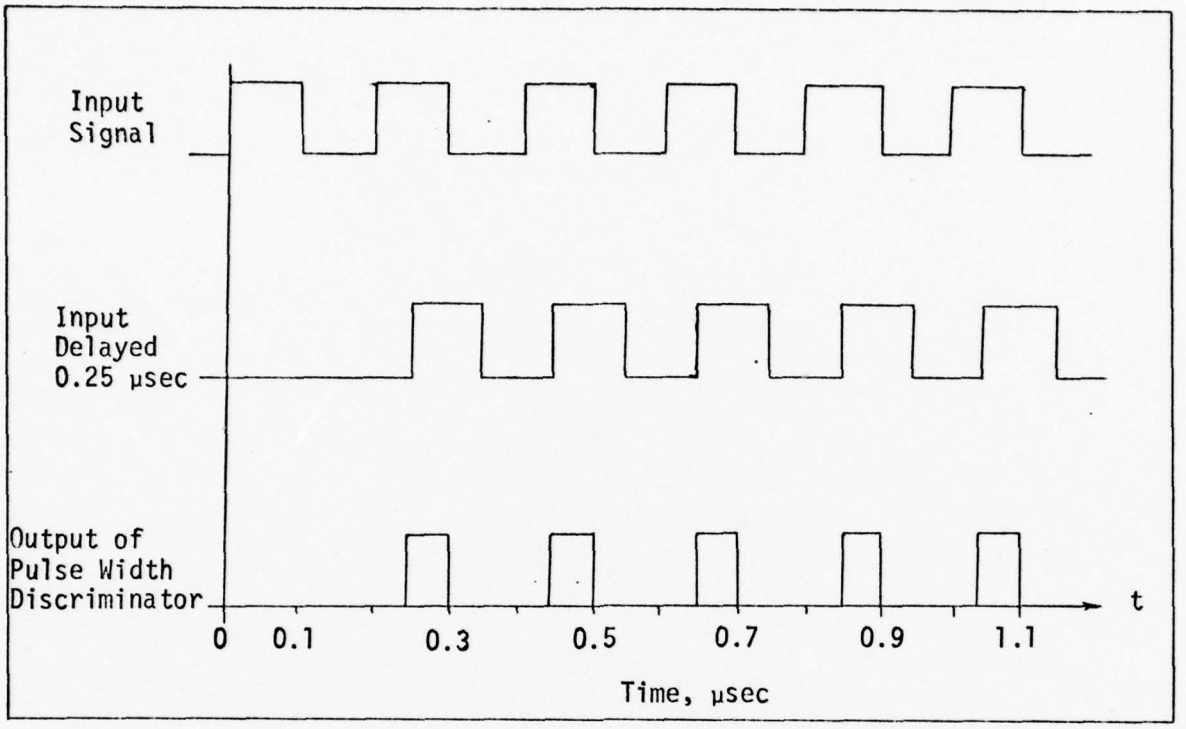

Fig 16. Decoding of Pulses Less Than 0.25 μsec

Noise Only: Wideband Signals

Interference signals whose bandwidths are greater than or equal to the overall receiver bandwidth were defined in Chapter 3 as wideband. With an overall receiver bandwidth of 5 MHz, the samples of the envelope process A(t) cannot vary over an interval of roughly 0.1 μsec. For the simulation, therefore, the samples that were input to the decoder as wideband signals were permitted to vary every 0.1 μsec.

In this section, the noise only case will be considered. This case includes those signal models that result from a sum of many transponder replies, with none dominant; and those signals that result from wideband noise jamming. The coherence time, τ_c, is fixed at 0.1 μsec. The performance statistic of interest is the probability of false alarm.

The results of the simulation for the wideband, noise-only case are presented in Table II. These results are tabulated in terms of noise power in dB above MTL. For each value of noise power, the confidence interval has been computed according to the Chernoff bound (reference Appendix B).

The results of Table II are shown in the form of a graph in Figure 17. The solid lines represent the confidence bounds (on the actual probability) that were obtained for a given number of observations and derived resultant probability. The actual values of probability of false alarm lie within the solid lines with 99% certainty. The dotted lines indicate the values of probability of false alarm that were experimentally derived.

It was stated in Chapter II that the transition of the input/output (I/O) curve of the logarithmic amplifiers (between the linear region and log region) occurs at 3dB above MTL. This point is indicated in Figure 17. All graphs of data presented in the remainder of this chapter will exhibit a discontinuity at this point. The discontinuity results from the implementation that was used to simulate this transition point.

The results from this case are best portrayed with the graph in Figure 18. This figure shows two separate curves, one for entirely linear receiver operation and one for entirely logarithmic operation. In the region of MTL to 3dB above MTL (where operation of a typical receiver is linear) the effects of the noise are significant. Likewise, in the region for signal powers greater than 6dB above MTL (where operation of the receiver is logarithmic) the effects of the noise are significant. It appears that the receiver characteristic accentuates the effects of the interference.

Figure 18 also shows the regions for which the noise has very little effect. Ideally it would be desirable for the receiver to operate in the log

Noise Power in Terms of MTL	Number of Observations	P_{fa}	Confidence Interval
-7 dB	39,849	0.00083	0.00043 to 0.0013
-4 dB	2,468	0.113	0.094 to 0.133
-2.6 dB	954	0.487	0.438 to 0.536
-1 dB	4,935	0.578	0.557 to 0.599
0 dB	2,468	0.691	0.663 to 0.719
1.5 dB	5,281	0.75	0.732 to 0.768
2 dB	4,935	0.76	0.741 to 0.778
3 dB (Linear)	2,628	0.72	0.693 to 0.746
3 dB (Log)	4,935	0.0087	0.005 to 0.013
5 dB	4,935	0.121	0.107 to 0.135
6 dB	2,468	0.308	0.280 to 0.337
9.5 dB	2,468	0.723	0.695 to 0.75
12 dB	2,468	0.691	0.663 to 0.719
14 dB	2,468	0.493	0.462 to 0.524
15.6 dB	2,468	0.35	0.321 to 0.379
17 dB	4,935	0.208	0.191 to 0.226
18 dB	4,935	0.136	0.121 to 0.151
19 dB	2,961	0.086	0.071 to 0.102

Table II. Noise-Only Wideband Results

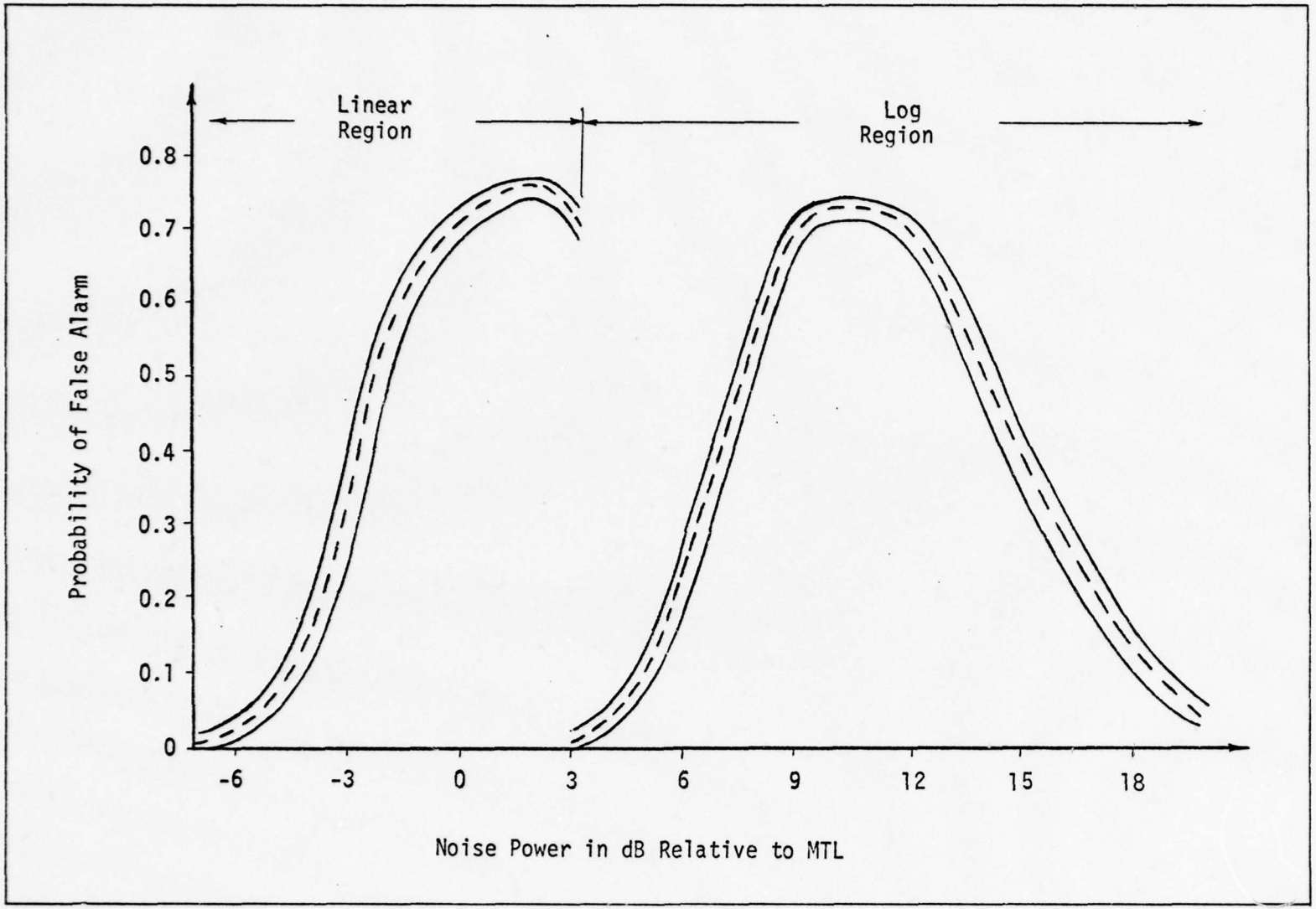

Fig 17. Wideband Interference Results

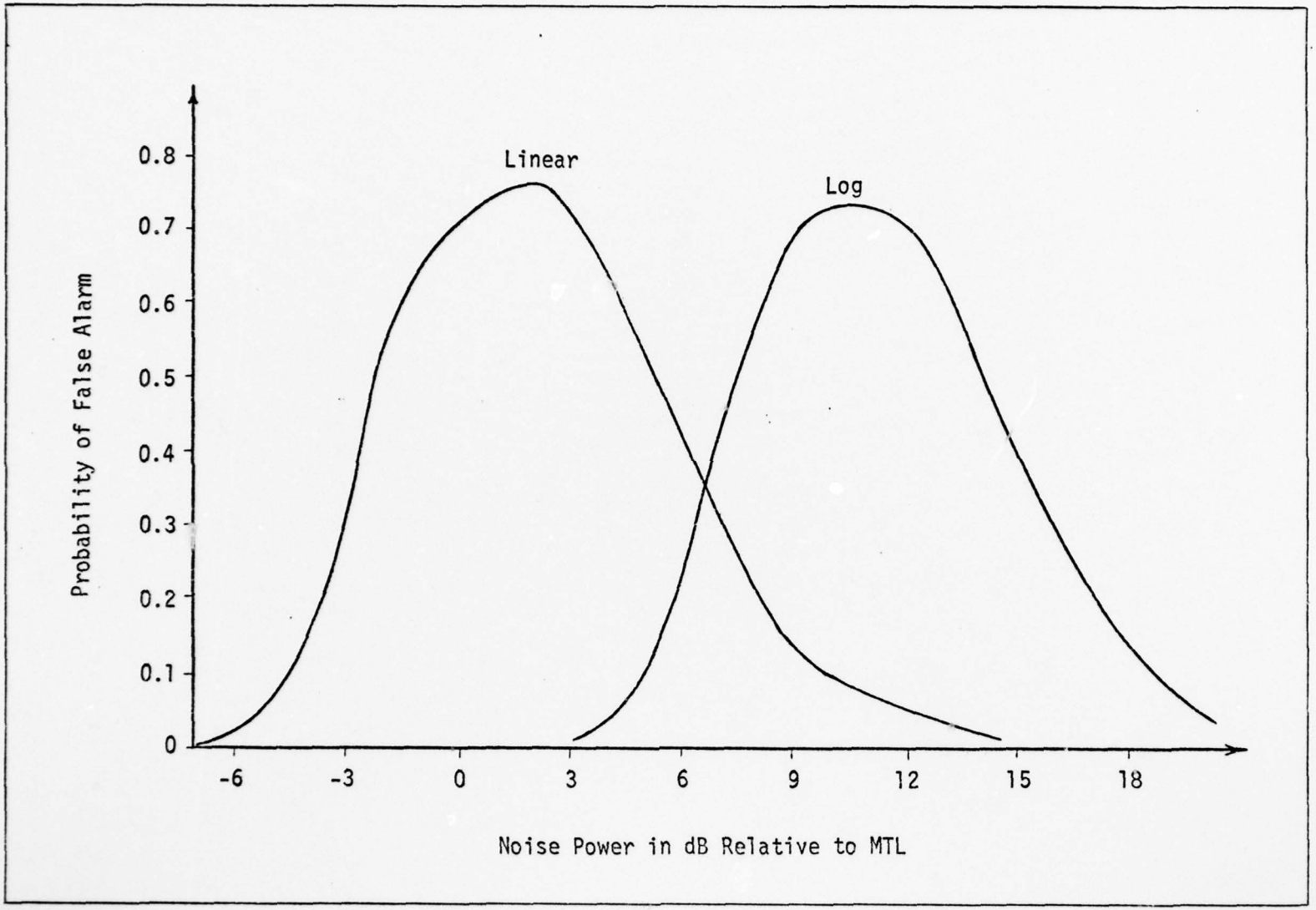

Fig 18. Wideband Interference Results, Extended Operating Regions

region to reduce the effects of low power interference (MTL to 3dB above MTL), and in the linear region for higher power interference (greater than 6dB above MTL).

Improvement of receiver performance against low power interference requires extending the input/output characteristic of the logarithmic amplifiers, so that the receiver operation is not linear in the region of MTL to 3dB above MTL. This type of change would require hardware modification, since the characteristics of the amplifiers are the result of the hardware with which they are built.

To improve performance against higher powered interference (greater than 6dB above MTL), it would be desirable to have the receiver operating in the linear region. However, linear receiver operation would limit the dynamic range of the receiver, unless some form of automatic gain control (AGC) was added to it.

Figure 17 and 18 show values of noise powers only up to 19dB above MTL. The dynamic range of an actual interrogator receiver is typically greater than this. However, both of these figures show that as the power of the interference becomes high (greater than 12dB above MTL) the effects of the interference decrease. This is because the decoder looks for pulses, and as the interference signal increases in power, the received signal no longer exhibits pulse-like tendencies. If the interference power is so great that the signal is consistently above MTL, the decoder interprets the interference as one very long pulse, and no false alarms are generated. Therefore, as the power of the interference increases above MTL + 12dB, the probability of false alarm decreases. In terms of intentional interference, this implies that increases in jammer power (above a certain level) will not provide increased jammer effectiveness. In terms of unintentional interference, this

implies that as the range of the N targets generating replies decreases (with respect to the interrogator), the probability of false alarm decreases. That is, replies from many near-range targets are less likely to false alarm the interrogator receiver.

Noise Only: Narrowband Signals

Interference signals whose bandwidths are less than the overall receiver bandwidth were defined in Chapter III as narrow band. The amplitude of the envelope process, A(t), that results from narrowband signals varies more slowly than 0.1 μsec. As in the previous section, the signals considered in this section are the result of either many transponder replies, with none dominant, or a random-pulse-type jammer. The difference is, however, that the correlation time, τ_c, for narrowband signals is greater than that for wideband signals (0.1 μsec).

It was stated in Chapter V that the correlation time for narrowband signals was modeled as a uniform random variable. The limits on the uniform distribution of τ_c determine the mean value of the correlation time. The results presented in this section will show how the performance of the interrogator receiver varies as a function of the mean correlation time. Two different sets of distribution limits were chosen for τ_c; uniform [0, 0.5 μsec] and uniform [0, 1.0 μsec]. The mean values of these two distributions are 0.25 μsec and 0.5 μsec, respectively. Probabilities of false alarm were determined for each of these two cases. The results of these two cases were then compared to the results from the wideband case, where the correlation time was fixed at 0.1 μsec.

Table III shows the results obtained for $E[\tau_c]$ = 0.25 μsec. Again, since there is no dominant signal component, the performance statistic is the

Noise Power Relative To MTL	Number of Observations	P_{fa}	Confidence Interval in % of Derived Probability
-4 dB	4,935	0.0574	0.048 to 0.068
-1 dB	2,468	0.21	0.186 to 0.235
0 dB	2,468	0.264	0.237 to 0.291
1.5 dB	2,961	0.25	0.226 to 0.274
2.0 dB	2,961	0.227	0.204 to 0.251
3.0 dB (Linear)	2,961	0.159	0.139 to 0.18
3.0 dB (Log)	3,948	0.012	0.007 to 0.018
4.77 dB	3,948	0.066	0.054 to 0.078
6 dB	3,948	0.14	0.124 to 0.157
9.5 dB	3,948	0.251	0.230 to 0.272
12 dB	3,948	0.15	0.133 to 0.168
14 dB	3,948	0.09	0.077 to 0.104
15.5 dB	3,948	0.0355	0.027 to 0.045
17 dB	3,948	0.016	0.01 to 0.022

Table III. Noise Only: Narrowband Signal Results, $E[\tau_c] = 0.25$ μsec.

probability of false alarm, P_{fa}. This table shows P_{fa} as a function of the interference power (in dB relative to MTL). As before, the confidence interval that was determined using the Chernoff bound is indicated.

Table IV shows the results obtained for $E[\tau_c]$ = 0.5 μsec. The format of this table is identical to that of Table III. By comparing Tables III and IV, one can see that P_{fa}'s for the case of $E[\tau_c]$ = 0.5 μsec are roughly one-half the P_{fa}'s for the case of $E[\tau_c]$ = 0.25 μsec (for comparable noise powers).

A compilation of the results of Tables II (wideband results), III, and IV (narrowband results) is shown in Figure 19. For clarity of presentation, the intervals of confidence are not shown on this graph, but they are included in Tables II, III, and IV.

Figure 19 shows that as $E[\tau_c]$ increases, P_{fa} decreases. This implies that as the coherence time (that is, the length of time over which a random signal is roughly constant) of the noise increases, the P_{fa} decreases. As the correlation time of a signal increases, that signal is less likely to exhibit the specific pulse-like tendencies required by the decoder. Thus, the interrogator receiver is less vulnerable to interference signals whose coherence time is greater than $\frac{1}{2B_{IF}}$ (i.e., narrowband signals).

Figure 19 also shows (for narrowband signals) that beyond a certain value of noise power, an increase in noise power results in lower P_{fa}'s. This is consistent with the phenomenon observed for wideband, noise-only signals.

Signal-Plus-Noise Results

Although the signal-plus-noise model is the most complex to analyze experimentally, it is probably the most realistic model that was considered.

Noise Power Relative to MTL	Number of Observations	P_{fa}	Confidence Interval in % of Derived Probability
-4 dB	4,935	0.033	0.0256 to 0.041
-1 dB	7,896	0.081	0.072 to 0.09
0 dB	8,390	0.083	0.074 to 0.09
1.5 dB	7,403	0.0692	0.06 to 0.078
2 dB	7,403	0.0593	0.051 to 0.068
3 dB (Log)	3,948	0.0056	0.0024 to 0.0095
4.7 dB	3,948	0.028	0.02 to 0.036
6 dB	3,948	0.072	0.06 to 0.085
9.5 dB	3,948	0.077	0.064 to 0.09
12 dB	3,948	0.043	0.034 to 0.053

Table IV. Noise Only: Narrowband Signal Results $E[\tau_c]$ = 0.5 μsec

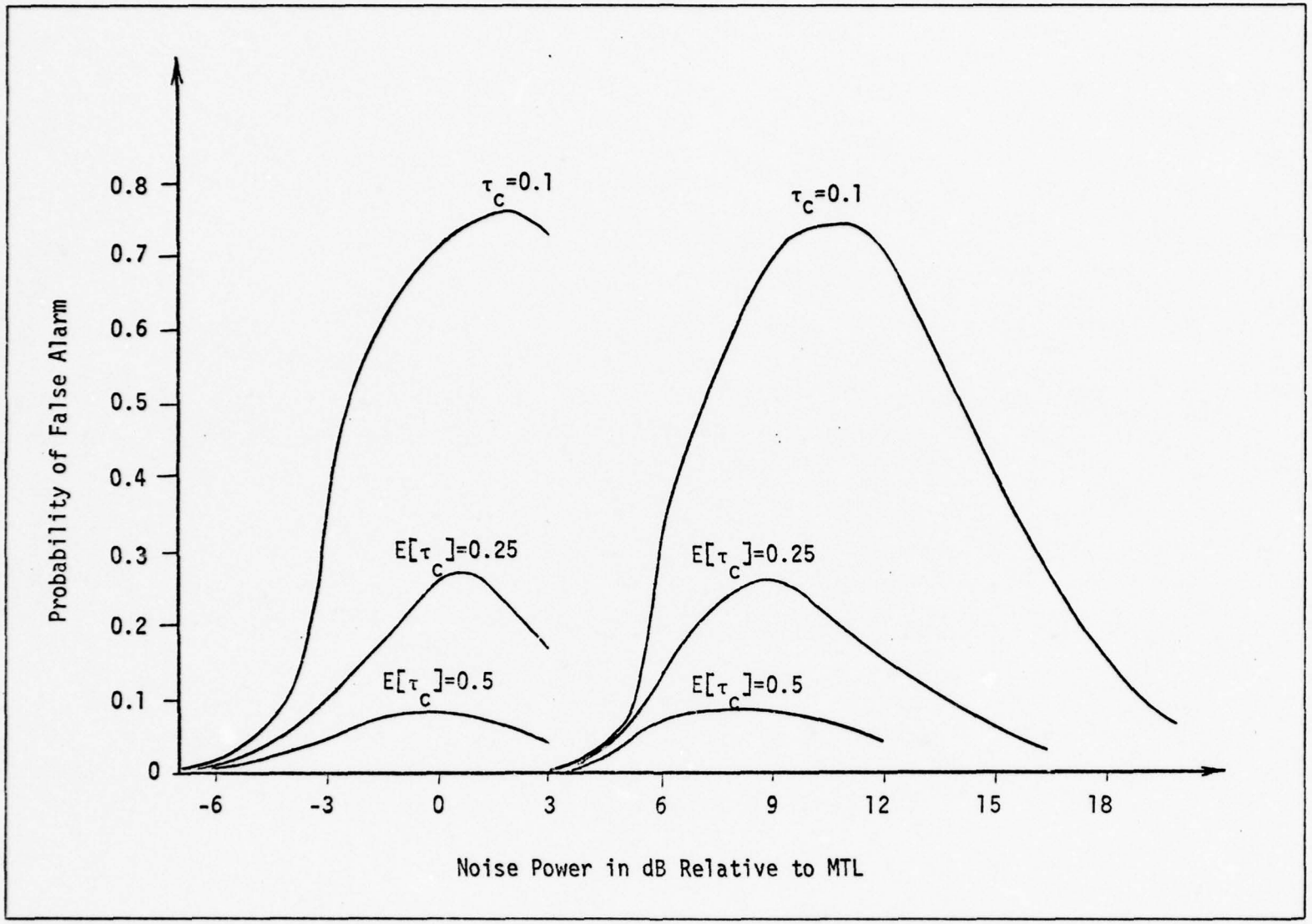

Fig 19. Narrowband Interference Results

For this case, the received signal consists of interference plus a valid reply. In terms of unintentional interference, this implies that there is one dominant reply among the N different replies received. In terms of intentional interference, this implies that a valid reply is present along with the jamming signal.

The performance statistic of interest for the signal-plus-noise case is the probability of error, P_E. One would intuitively expect P_E to be a function of not only the interference power, but the signal power as well. Many different combinations of signal power and interference power are possible. It was the objective of this portion of the study only to establish relative trends in the P_E as signal power and interference power were varied.

The results presented in this section include only wideband interference. No data was collected for the signal-plus-narrowband-interference case. It was shown in previous sections of this chapter that the interrogator receiver is more vulnerable to wideband interference than to narrowband interference. It will be assumed that this is true for the signal-plus-noise case as well. The reader is cautioned, however, that this in only an assumption, the validity of which can be determined through future study.

The results for this case are presented in Figures 20 and 21. Figure 20 shows results for the linear receiver operating region (i.e., low interference power and low signal power). Figure 21 shows results for logarithmic receiver operation (i.e., high interference power and/or high signal power). Values of P_E are plotted versus interference powers (relative to MTL) for specific values of signal power (also relative to MTL). This data is not tabulated, because it is too voluminous to list.

These figures do not indicate any intervals of confidence, because only a limited number of observations were made for each data point. The con-

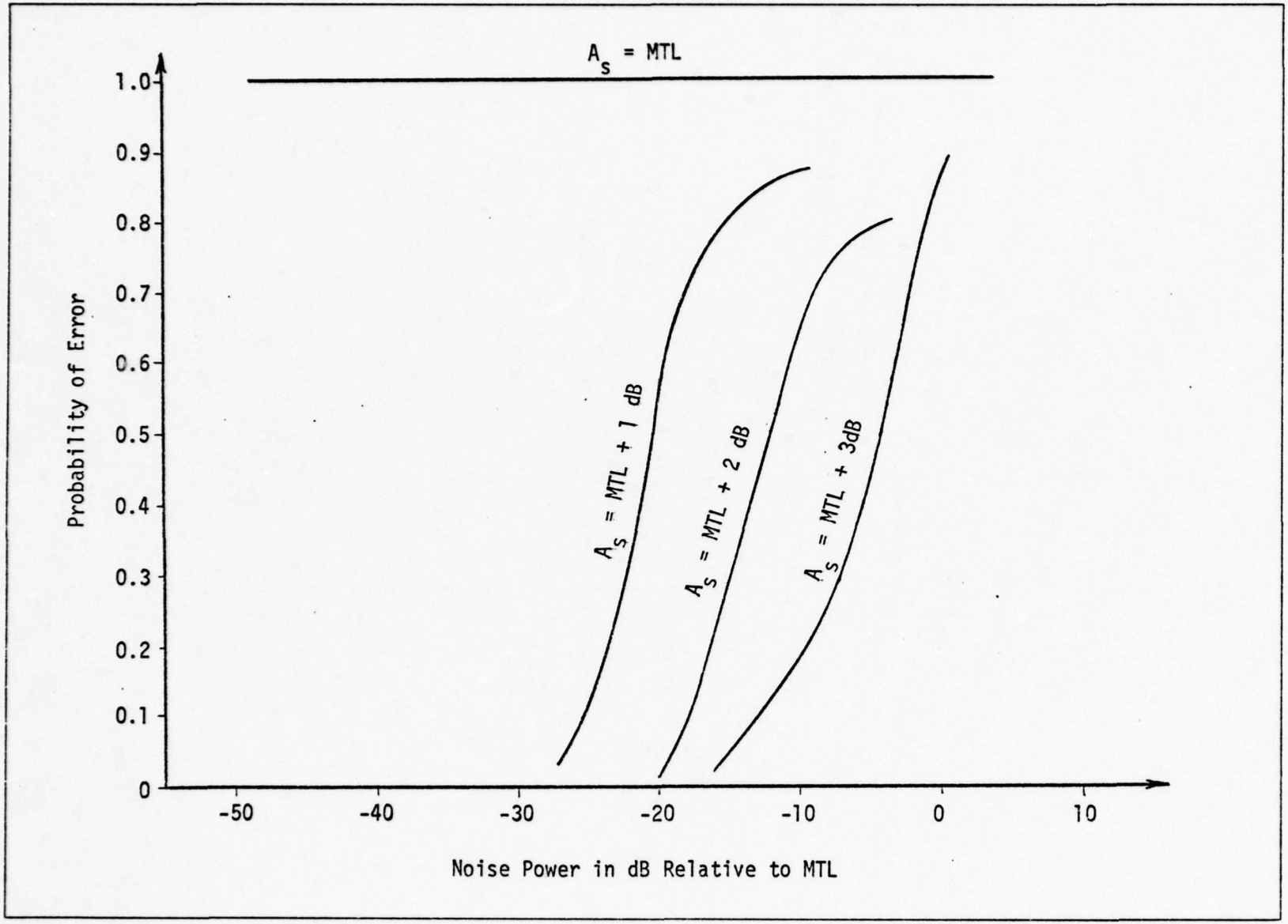

Fig 20. Signal-Plus-Noise Results: Linear Operating Region

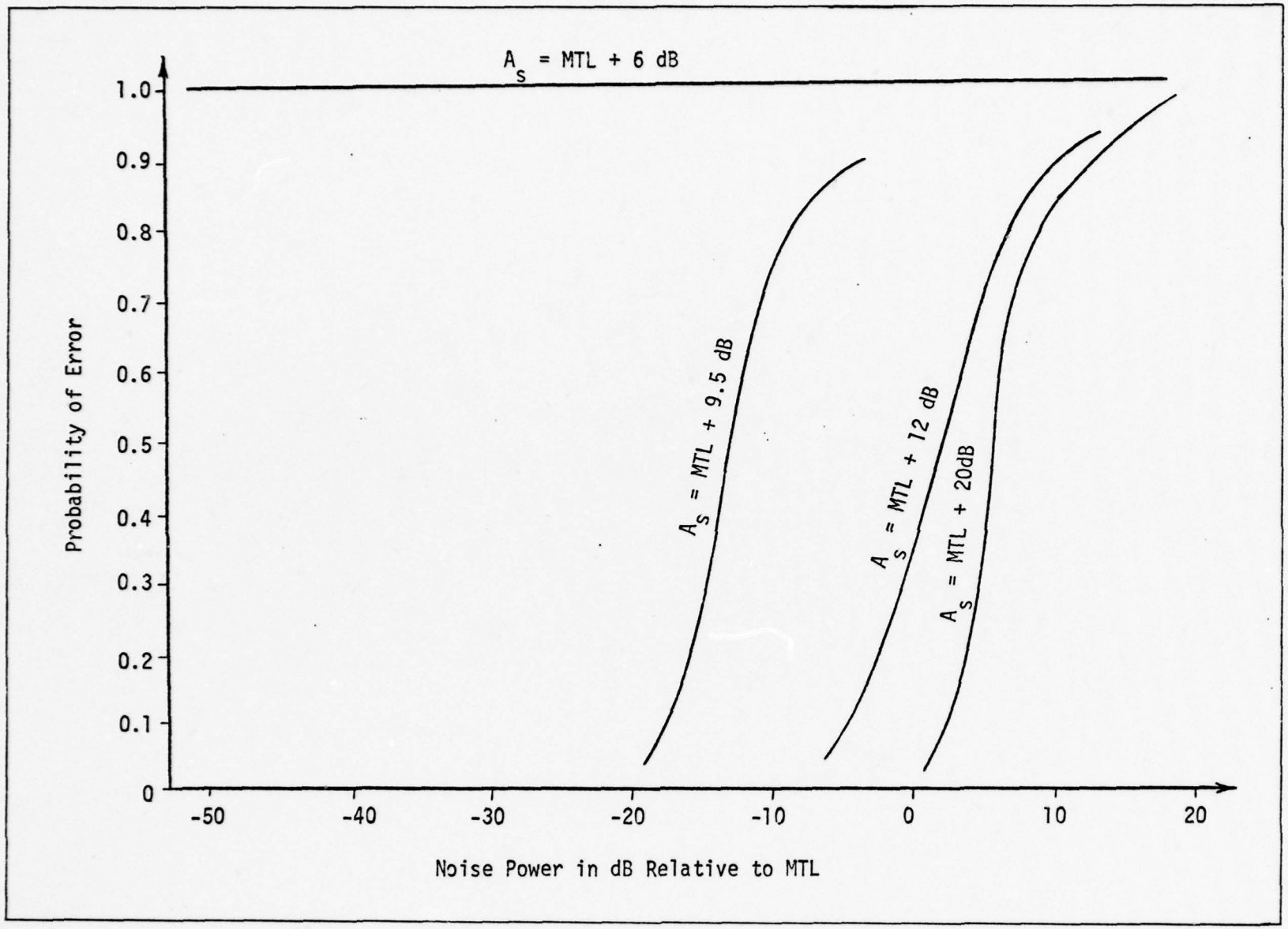

Fig 21. Signal-Plus-Noise Results: Log Operating Region

sistency of the data, however, attests to validity of these results, in spite of the limited number of observations that were made (usually 304).

The most obvious conclusion one can draw from these figures is that when the signal is at MTL, just about any value of interference power will prevent the valid reply from being detected. This result is not startling, since most radar systems experience this phenomenon.

Basically, Figures 20 and 21 indicate that as the power in the signal increases, more noise power is required to maintain a constant P_E. This is true, however, only up to a point. When the signal power increases above MTL plus 20dB, no increase in interference power is necessary to maintain a specific P_E. Results obtained for signal powers of MTL + 26dB and MIL + 40dB were nearly identical to those obtained for a signal power of MTL +20dB.

The reason that such a limit exists is not attributable to the relationship of signal power to MTL, or even signal power to interference power. Rather, it is the value of interference power relative to MTL that is the governing factor. At low signal power levels, the interference effects a valid reply as shown in Figure 22. Effective interference brings a part or all of a pulse below MTL. This distorts the pulse characteristics of the valid reply (as received by the interrogator) and can prevent detection. At high signal power levels (i.e., greater than MTL + 20dB), the effects of the interference raise the baseline of the valid reply above MTL, causing the decoder to interpret the signal as one, very long pulse. (This phenomenon was discussed earlies in this chapter.) Figure 23 illustrates this condition.

Finally, Figure 21 can be used to generalize the results of the signal-plus-noise case. Regardless of the power in the valid reply, interference with power levels in the region of 10dB above MTL will effectively mask 80%

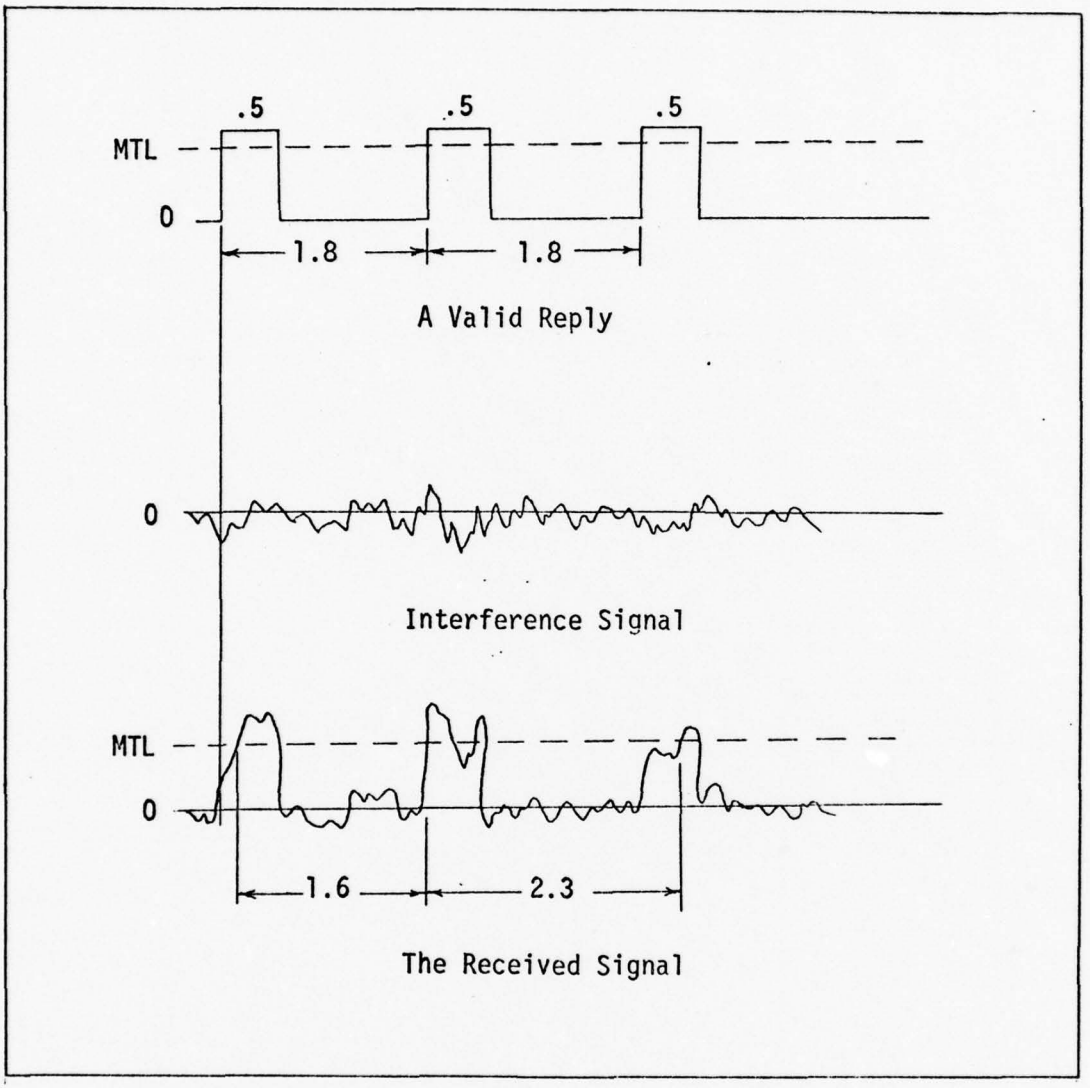

Fig 22. Interference Effect for Low Signal Power

of the valid replies being received by the interrogator.

Summary

The results presented in this chapter indicate that the maximum decode rate of the interrogator receiver can be realized with a number of different periodic pulse-type formats. It was shown that the pulse length discriminator of the decoder will not always reject pulses less than a specified width.

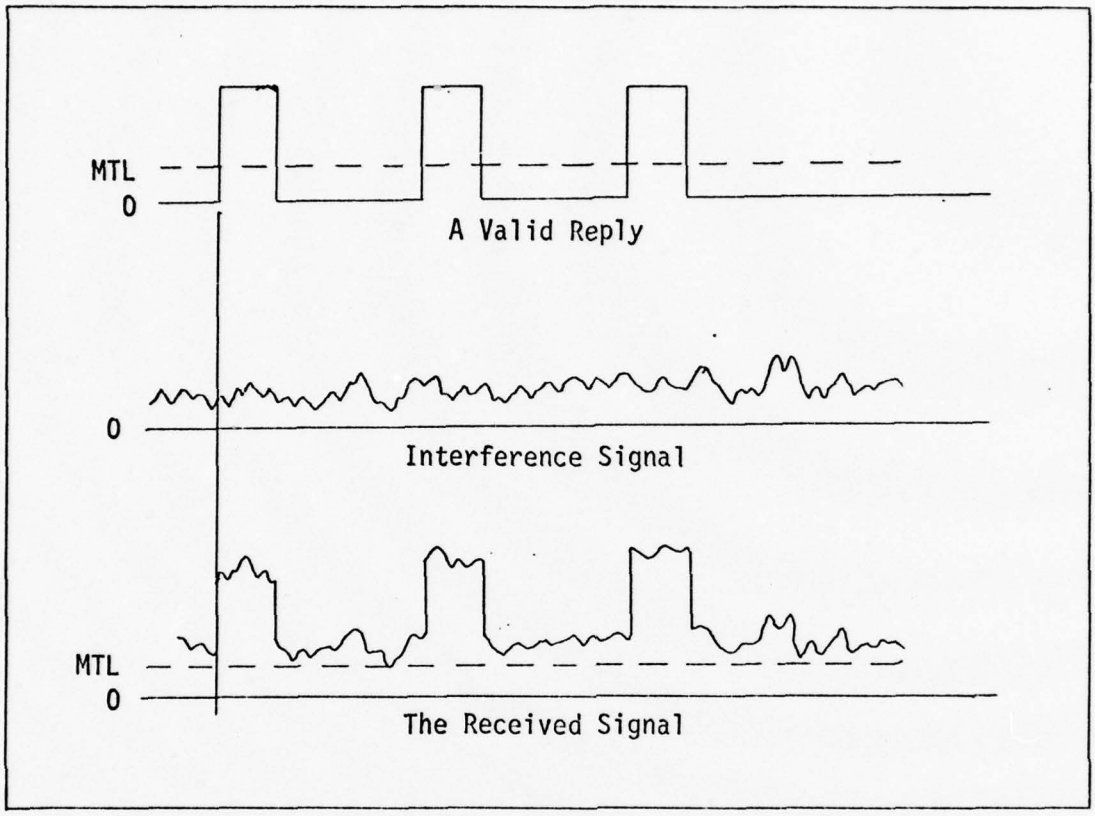

Fig 23. Interference Effect for High Signal Power

For the noise-only case, the results show that P_{fa}'s for wideband interference are higher than P_{fa}'s for narrowband interference. It was observed that beyond a certain point, increases in interference power result in decreases of P_{fa} for both wideband and narrowband interference.

Finally, for the signal-plus-noise case, the results indicated that for interference powers in the region of 10dB above MTL, a valid reply will be masked, regardless of the power in that valid reply.

VII. Conclusions and Recommendations

In this study, the vulnerability of a typical IFF interrogator to wideband and narrowband interference signals were investigated. In general, many types of fixed periodic pulse signal formats will result in the maximum decode rate of the interrogator receiver. For a certain class of periodic pulse signals, the pulse width discriminator of the decoder will not effectively reject pulses whose widths are less than a specified value.

Zero-mean, Gaussian processes with uncorrelated quadrature components were used to model various types of random interference. Wideband interference signals (signals of bandwidth greater than 10 MHz) produced probabilities of false alarm that were higher than those for narrowband interference signals. In both cases, once the interference power increases beyond a certain point, the probability of false alarm decreases.

The operating characteristic of the interrogator receiver tends to maximize the effects of the interference, when the power of the interference is in the region of MTL to 20dB above MTL. Linear receiver operation in the region of MTL to 3dB above MTL is the worst case in terms of the receiver. Likewise, logarithmic receiver operation in the region of 3dB above MTL to 19dB above MTL is worst case for the receiver. The operating characteristic of a typical interrogator receiver is, however, linear in the region of MTL to 3dB above MTL, and logarithmic above MTL + 3dB.

When a valid reply is present along with the interference, the performance of the decoder is a function of signal (valid reply) power as well as interference power, up to a point. As the power in the valid reply signal increases,

the performance of the interrogator receiver increases until the power of the signal reaches 20dB above MTL. Beyond this point, further increases in signal power do not result in increased performance.

The performance of the interrogator receiver modeled in this study could be improved if the pulse width discriminator would effectively reject pulses of widths less than 0.25 μsec. This would make the decoder less vulnerable to wideband interference signals. A fix of this type would most likely require a pulse width discriminator that is different than the one used in the decoder modeled here.

The logarithmic amplifiers in the interrogator receiver serve to increase the dynamic range of the receiver. Logarithmic receiver operation, however, results in poorer performance than linear receiver operation. If the receiver were made entirely linear, some form of automatic gain control (AGC) would be necessary to provide the dynamic range required.

An AGC circuit might also improve the signal-plus-noise performance of the receiver. Basically, an AGC circuit would result in a "floating" threshold, which would provide improved performance with increasing signal (valid reply) power.

Bibliography

1. Abd-Alla, A. M., and A. C. Meltzer. Principles of Digital Computer Design, Volume 1. New Jersey, Prentice-Hall, Inc., 1976.

2. Blake, I. F., and W. C. Lindsey. "Level Crossing Problems For Random Processes", IEEE Transactions on Information Theory, IT-19(3): 295-315, May 1973.

3. Davenport, W. B., Jr. Probability and Random Process: An Introduction for Applied Scientists and Engineers. New York: McGraw-Hill Book Company, 1970.

4. Highleyman, W. H. "The Design and Analysis of Pattern Recognition Experiments", The Bell System Technical Journal, 41 (2): 723-744, March 1962.

5. "Logic IV, Logic Simulation & Fault Analysis", Future Avionics Through Computer Aided Technology, Users Manual, Volume 3. Prepared for the Air Force Avionics Laboratory by the Westinghouse Electric Corporation. Published under authority of the Secretary of the Air Force, 1 April 1977.

6. Lyons, B. W. A Speckle Noise Model for Optical Heterodyne Line-Scan Imagery. MS Thesis. Wright-Patterson AFB, Ohio: Air Force Institute of Technology, 1977.

7. Middleton, D. An Introduction to Statistical Communication Theory. New York: McGraw-Hill Book Company, Inc.; 1960.

8. Papoulis, A. Probability, Random Variables, and Stochastic Processes. New York: McGraw-Hill Book Company, 1965.

9. Payne, W. H., J. R. Rabung, and T. P. Bogyo. "Coding the Lehmer Pseudo-Random Number Generator", Communications of the ACM, 12 (2): 85-86 (February 1969).

10. Rice, S. O. "Mathematical Analysis of Random Noise" The Bell System Technical Journal, 24 (1): 46-156 (January, 1945).

11. Schwartz, M. Information Transmission, Modulation, and Noise (Second Edition). New York: McGraw-Hill Book Company, 1970.

12. Wozencraft, J. M. and I. M. Jacobs. Principles of Communications Engineering. New York: John Wiley & Sons, Inc., 1965.

13. Ziemer, R. E. and W. H. Tranter. Principles of Communications: Systems, Modulation, and Noise. Boston: Houghton Mifflin Company, 1976.

Appendix A

LOGIC 4

The LOGIC 4 Logic Simulation and Fault Analysis Program was prepared for the Air Force Avionics Laboratory (AFAL) by the Westinghouse Electric Corporation under contract F33615-76-C-1183. This program is part of the Computer Aided Design (CAD) capability at AFAL. This appendix provides only a brief description of its use and application relative to this study. Additional information can be found in Reference 5.

LOGIC 4 is capable of performing many useful functions for logic circuit design and evaluation. Of particular interest to this study is its ability to simulate any part or all of a logic circuit. Given an input signal, LOGIC 4 will simulate the stimulus/response characteristics of each element in the circuit.

To use the LOGIC 4 simulation capability, one must define the elements of the circuit and their respective interconnection. The LOGIC 4 program can simulate simple logic elements (such as NOR, NAND, flip-flop, delay lines and one-shots) as well as more complex logic elements (such as shift registers). Input signals are defined as the EXTERNALS, and are specified in terms of 1's and 0's. LOGIC 4 simulates the logic circuit operation that results from a given external. The outputs of the LOGIC 4 simulation are typically presented on a timing diagram that shows the state of circuit elements of interest at specified times.

The specific decoder model that was simulated is shown in Figure 24. This diagram was obtained from Figure 13 by combining the operations of some of the logic elements using DeMorgan's Theorem (Ref 1:101). All of the elements are assumed to be zero-delay, that is, a change in the input to an element results in an instantaneous change in the ouput (if a change is to occur).

The smallest unit of time in a LOGIC 4 simulation is defined as a gate time. The delay times of the delay lines and the on-times of the one-shots are specified in terms of the gate time. A coarse time is a user defined multiple of the gate time. For this study, one coarse time was defined to be equal to two gate times. With the coarse time scaled to represent 0.1 μsec, a delay of 1.8 μsec implies a delay of 36 gate times. Likewise, the other delays and on-times (of one-shots) can be expressed in terms of an integer number of gate times.

The externals (input 1's and 0's) are derived in a subroutine that is not part of the LOGIC 4 program. The LOGIC 4 program accepts a new input every gate time, although the value of the input signal can change only every coarse time. With a ratio of two gate times/coarse time, it was required to keep a particular input constant for at least 2 gate times (=1 coarse time), which was the shortest correlation time permitted by the bandwidth limitations of the receiver.

Although LOGIC 4 can provide a timing diagram showing the outputs of all circuit elements, only the output of the last one-shot was recorded. These outputs were passed to an external subroutine for determination of appropriate performance statistics (P_{fa} or P_E).

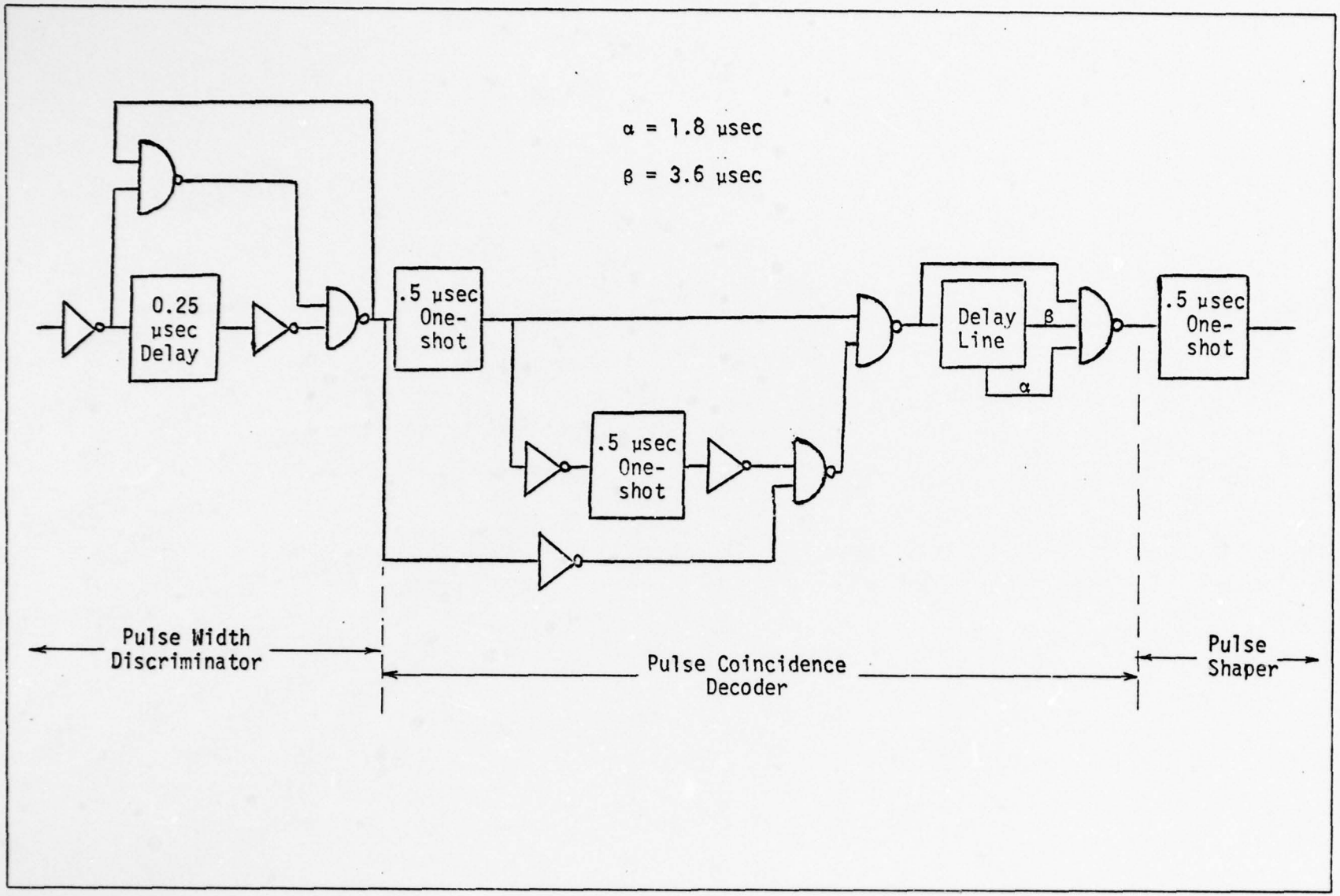

Fig 24. Decoder Model for LOGIC 4

Appendix B

Determination of Confidence Intervals: The Chernoff Bound

This appendix derives analytic expressions that can be used to determine confidence intervals on probabilities of false alarm and probabilities of error that have been experimentally determined.

A probability of false alarm or error can be derived experimentally using

$$P^* = \frac{1}{N} \sum_{i=1}^{N} x_i \tag{66}$$

where N is the number of observations and

$$x_i = \begin{cases} 1; & \text{if the } i^{th} \text{ observation was a false alarm or error} \\ 0; & \text{otherwise.} \end{cases} \tag{67}$$

In general, the x_i's are random variables with identical probability density functions p_x, means $E[x]$, and variances σ_x^2. As N gets very large, the value of P* (now a random variable) approaches the actual probability, P. In essence, the probability P is being approximated by the relative frequency of occurrence of a false alarm or error. The fact that this relative frequency of occurrence does indeed approach the actual probability desired is based on the assumption of stability of averages (Ref 3:10). The assumption of stability of averages is based simply on empirical observations that have been made in physical experiments.

The error between the derived probability and the actual probability can be expressed as

$$\varepsilon_p = \left| P^* - P \right| \tag{68}$$

With the assumption of stability of averages, $P = E[P^*]$. Then Eq (68) becomes

$$\varepsilon_p = \left| P^* - E[P^*] \right| \tag{69}$$

$$= \left| \frac{1}{N} \sum_{i=1}^{N} x_i - E\left[\frac{1}{N} \sum_{i=1}^{N} x_i \right] \right| \tag{70}$$

$$= \left| \frac{1}{N} \sum_{i=1}^{N} x_i - \frac{1}{N} \sum_{i=1}^{N} E[x_i] \right| \tag{71}$$

$$= \left| \frac{1}{N} \sum_{i=1}^{N} x_i - E[x_i] \right| \tag{72}$$

$$= \left| \frac{1}{N} \sum_{i=1}^{N} y_i \right| \tag{73}$$

where the y_i are now zero-mean random variables with variances $\sigma_y^2 = \frac{\sigma_x^2}{N}$ and identical probability density functions, p_y (Ref 12:96). The probability that the error, ε_p, exceeds an arbitrary value ε is

$$P[\varepsilon_p \geq \varepsilon] = P\left[\left| P^* - P \right| \geq \varepsilon \right] \tag{74}$$

$$= P\left[\frac{1}{N} \sum_{i=1}^{N} y_i \geq \varepsilon \right] \tag{75}$$

At this point, it is convenient to introduce the random variable, z, which is defined to be a binary-valued function of $\sum_{i=1}^{N} y_i$:

$$z = f(y_i) = \begin{cases} 1 \; ; & \left| \sum_{i=1}^{N} y_i \right| \geq \alpha \\ 0 \; ; & \left| \sum_{i=1}^{N} y_i \right| < \alpha \end{cases} \tag{76}$$

Comparison of Eq (75) and Eq (76) shows that

$$P\left[\left| \frac{1}{N} \sum_{i=1}^{N} y_i \right| \geq \varepsilon \right] = P\left[\left| \sum_{i=1}^{N} y_i \right| \geq N\varepsilon \right] = P[z = 1] \tag{77}$$

where α in Eq (76) is taken to be $N\varepsilon$. Since z can take on only the values 0 and 1,

$$E[z] = 0 \cdot P[z = 0] + 1 \cdot P[z = 1] \tag{78}$$

$$= P[z = 1] \tag{79}$$

Then, from Eq (77)

$$E[z] = P\left[\left| \frac{1}{N} \sum_{i=1}^{N} y_i \right| \geq \varepsilon \right] = E\left[f\left(\sum_{i=1}^{N} y_i \right) \right] \tag{80}$$

There is no simple way of evaluating $E\left[f\left(\sum_{i=1}^{N} y_i \right) \right]$ for an arbitrary p_y. Graphically, however, one can see that a bound can be placed on the function $f(\cdot)$. Figure 25 shows one such bound that is often used. For this case, $f(u) \leq \left(\frac{u}{N\varepsilon}\right)^2$. Using this function, $E\left[f\left(\sum_{i=1}^{N} y_i \right) \right]$ is bounded by the expression

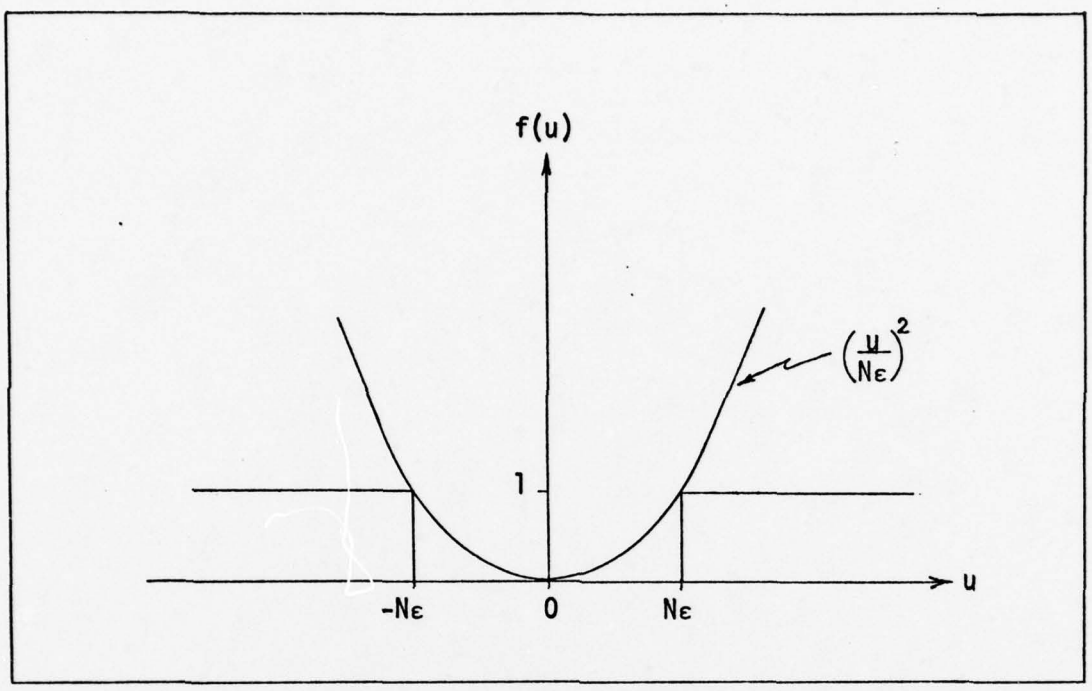

Fig 25. The "Weak Law" Bound

$$E\left[f\left(\sum_{i=1}^{N} y_i\right)\right] \leq E\left[\left(\frac{\sum_{i=1}^{N} y_i}{N\epsilon}\right)^2\right] = \left(\frac{1}{N\epsilon}\right)^2 E\left[\left(\sum_{i=1}^{N} y_i\right)^2\right] \tag{81}$$

Since the y_i are statistically independent, zero-mean, identically distributed random variables,

$$E\left[\left(\sum_{i=1}^{N} y_i\right)^2\right] = \sum_{i=1}^{N} \sigma_{y_i}^2 = N\sigma_y^2 \tag{82}$$

where σ_y^2 is the variance of one of the y_i random variables. Therefore,

$$E\left[f\left(\sum_{i=1}^{N} y_i\right)\right] \leq \left(\frac{1}{N\epsilon}\right)^2 N\sigma_y^2 = \frac{\sigma_y^2}{N\epsilon^2} \tag{83}$$

and thus

$$P\left[\left|\frac{1}{N}\sum_{i=1}^{N} y_i\right| \geq \varepsilon\right] \leq \frac{\sigma_y^2}{N\varepsilon^2} \tag{84}$$

This result is known as the Weak Law of Large Numbers. This expression can be used to determine the number of observations, N, that are necessary to bound the error ε_p to $\pm\varepsilon$, given the variance, σ_y^2.

In general, any function, $v_o(u)$, that satisfies

$$f(u) \leq v_o(u) \quad ; \quad \text{for all } u \tag{85}$$

can be used to bound $P\left[\left|\frac{1}{N}\sum_{i=1}^{N} y_i\right| \geq \varepsilon\right]$. Thus,

$$P\left[\left|\frac{1}{N}\sum_{i=1}^{N} y_i\right| \geq \varepsilon\right] \leq E\left[v_o\left(\sum_{i=1}^{N} y_i\right)\right] \tag{86}$$

where $f(u) \leq v_o(u)$ for all u.

An especially powerful function that has been used (Ref 12:99) to bound the positive half of f(u) is

$$h(u) = e^{\lambda(u - N\varepsilon)} \quad ; \quad \lambda \geq 0, \ \varepsilon \geq 0 \tag{87}$$

This function is shown in Figure 26. The curve of $\left(\frac{u}{N\varepsilon}\right)^2$ is also shown on this figure to show that h(u) does indeed provide a tighter bound.

Using this function, the expression for E[z] becomes

$$E[z] \leq E\left[e^{\lambda\left(\sum_{i=1}^{N} y_i - N\varepsilon\right)}\right]\Bigg|_{\lambda = \lambda_o} \tag{88}$$

where λ_o is the value of λ that minimizes the right side of the inequality.

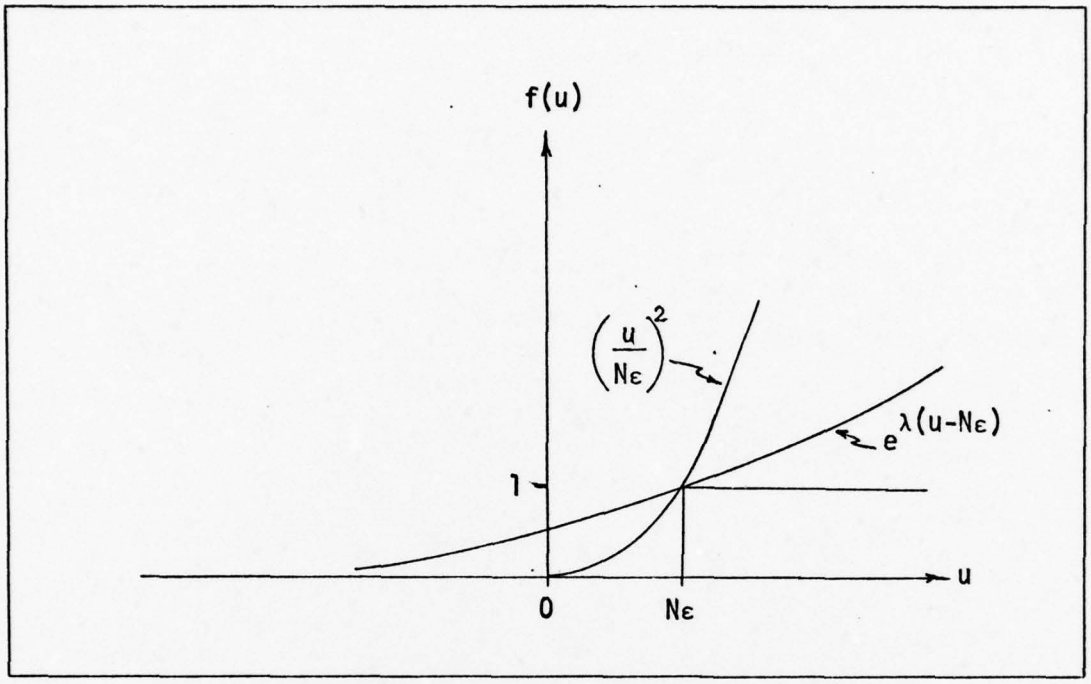

The Positive Half Bound

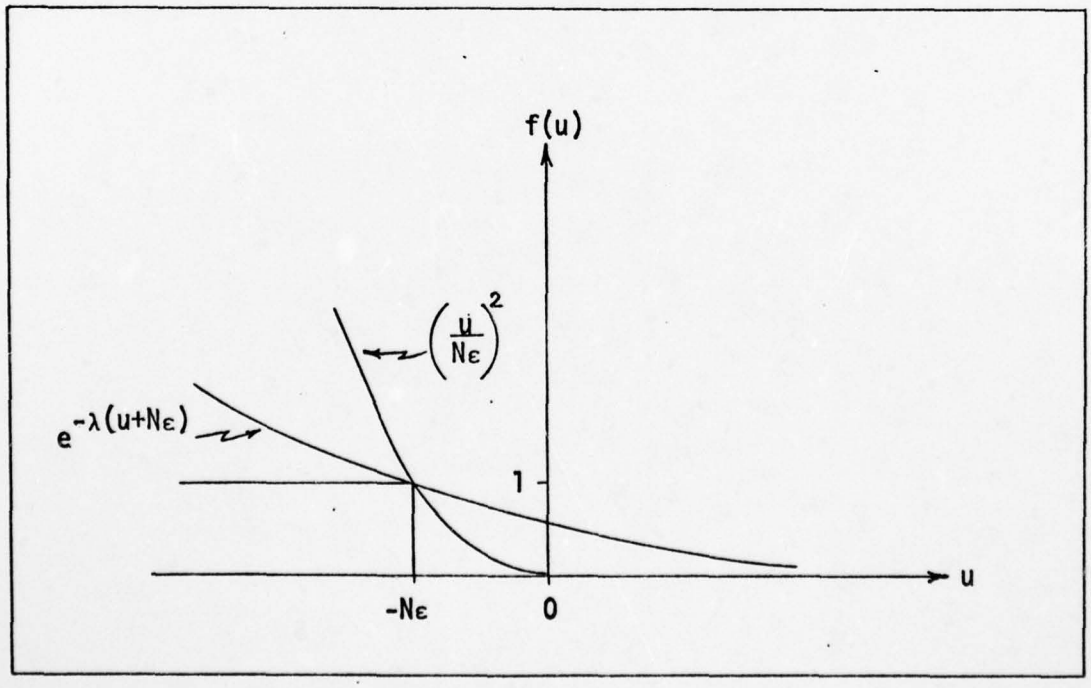

The Negative Half Bound

Fig 26. The Chernoff Bound

Then

$$P\left[\frac{1}{N}\sum_{i=1}^{N} y_i \geq \varepsilon\right] \leq E\left[\exp \lambda_o\left(\sum_{i=1}^{N} y_i - N\varepsilon\right)\right] \quad ; \quad \varepsilon \geq 0 \tag{89}$$

The right side of Eq (89) is known as the Chernoff bound.

With the assumptions that the y_i are zero-mean, identically distributed, statistically independent random variables, Eq (89) is reduced to

$$P\left[\frac{1}{N}\sum_{i=1}^{N} y_i \geq \varepsilon\right] \leq \left[E[\exp \lambda_o(y - \varepsilon)]\right]^N \quad ; \quad \varepsilon \geq 0 \tag{90}$$

where y here is equivalent to one of the identically distributed y_i.

It is convenient to express Eq (90) in terms of the variable, X, which is defined by

$$X = \ln\left[E[\exp \lambda_o(y - \varepsilon)]\right] \quad ; \quad \varepsilon \geq 0 \tag{91}$$

Then Eq (90) becomes

$$P\left[\frac{1}{N}\sum_{i=1}^{N} y_i \geq \varepsilon\right] \leq e^{-NX} \quad ; \quad \varepsilon \geq 0 \tag{92}$$

A similar expression can be derived that represents a bound for the negative half of f(u). In this case,

$$P\left[\frac{1}{N}\sum_{i=1}^{N} y_i < \varepsilon\right] \leq e^{-NX} \quad ; \quad \varepsilon < 0 \tag{93}$$

$$X = \ln\left[E[\exp \lambda_o(y - \varepsilon)]\right] \quad ; \quad \varepsilon < 0 \tag{94}$$

In terms of the actual probability, P, and the experimentally derived probability, P*, it can be shown that (Ref 12:102-103):

$$P_{c+} = P\left[P^* \geq d \right] = \left[\left(\frac{P^*}{d}\right)^{d} \left(\frac{1 - P^*}{1 - d}\right)^{1-d} \right]^{N} \quad ; \quad 1 \geq d \geq P \tag{95}$$

and

$$P_{c-} = P\left[P^* < d \right] = \left[\left(\frac{P^*}{d}\right)^{d} \left(\frac{1 - P^*}{1 - d}\right)^{1-d} \right]^{N} \quad ; \quad 0 \leq d < P \tag{96}$$

where

$$d = P + \varepsilon \quad ; \quad \text{for all } \varepsilon \tag{97}$$

The values of d can be interpretted as bounds around the actual probability, P. The above expressions can be used to determine the probability that the derived probability, P*, is outside an interval of $\pm\varepsilon$ around the actual probability, P, for a given number of observations. Usually, one is not afforded the luxury of making an arbitrarily large number of observations. Thus, Eq (95) and (96) are most often used to determine the values of d that can be realized with a finite number of observations (N); given P*, P_{c+}, and P_{c-} (typically, P_{c+} and P_{c-} are chosen to be equal). Figure 27 shows this relationship for various values of N, P*, and P. P_c ($= P_{c+} = P_{c-}$) is taken to be 0.05, which implies 95% confidence in these values. This figure agrees with a plot of the 95 per cent confidence intervals for a binomially distributed random variable, documented in an article by W. H. Highleyman (Ref 4:726).

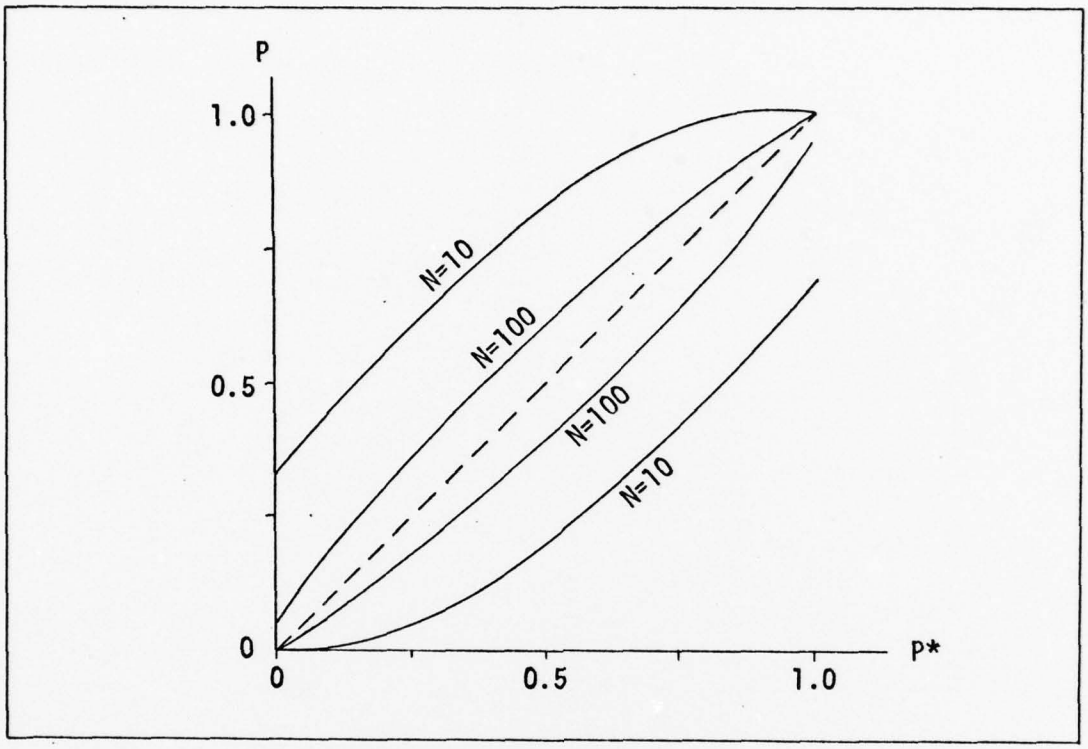

Fig 27. Confidence Bounds for P_c = 0.05

In general, Eq (95) and (96) can be used to determine d for any set of specific values of P_c, P*, and N. These values (of d) represent a confidence interval within which the actual probability of interest can be expected to lie (with 1 - P_c confidence).

VITA

Gregory S. Douple was born on 26 March 1950 in Reading, Pennsylvania, the son of Stanley R. and Gladys L. Douple. He graduated from high school in Fairborn, Ohio in 1968 and received a Bachelor of Science degree in Aerospace Engineering from the University of Cincinnati, Cincinnati, Ohio in 1973. He has worked as a Flight Test Director with the 4950th Test Wing, Wright-Patterson AFB, Ohio from June 1969 to August 1977. In September of 1977, he attended the Air Force Institute of Technology, where he received the Master of Science in Electrical Engineering in June 1978. He is a member of Tau Beta Pi, Eta Kappa Nu, Sigma Gamma Tau, the Association of Old Crows, and is a Professional Engineer-in-Training.

Permanent address: 1440 Poplar Drive
Fairborn, Ohio 45324

AD-A058 516 AIR FORCE INST OF TECH WRIGHT-PATTERSON AFB OHIO SCH--ETC F/G 17/7
AN INVESTIGATION INTO THE VULNERABILITY OF A TYPICAL IDENTIFICA--ETC(U)
JUN 78 G S DOUPLE

UNCLASSIFIED AFIT/GE/EE/78-13 NL

2 OF 2
AD
A058516

END
DATE
FILMED
11-78
DDC

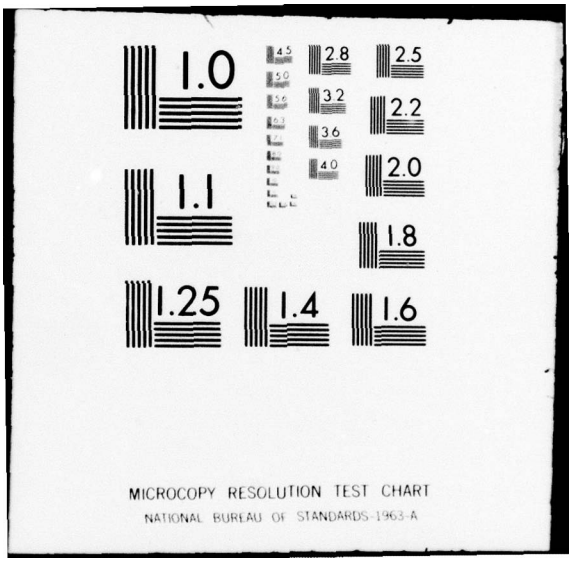
1.0
1.1
1.25
1.4
1.6
1.8
2.0
2.2
2.5
2.8
3.2
3.6
4.0
4.5
5.0
5.6
MICROCOPY RESOLUTION TEST CHART
NATIONAL BUREAU OF STANDARDS-1963-A

SECURITY CLASSIFICATION OF THIS PAGE *(When Data Entered)*

REPORT DOCUMENTATION PAGE		READ INSTRUCTIONS BEFORE COMPLETING FORM
1. REPORT NUMBER: AFIT/GE/EE/78-13 ✓	2. GOVT ACCESSION NO.	3. RECIPIENT'S CATALOG NUMBER
4. TITLE *(and Subtitle)*: AN INVESTIGATION INTO THE VULNERABILITY OF A TYPICAL IDENTIFICATION FRIEND OR FOE (IFF) INTERROGATOR RECEIVER		5. TYPE OF REPORT & PERIOD COVERED: MS Thesis 6. PERFORMING ORG. REPORT NUMBER
7. AUTHOR(s): Gregory S. Douple		8. CONTRACT OR GRANT NUMBER(s)
9. PERFORMING ORGANIZATION NAME AND ADDRESS: Air Force Institute of Technology (AFIT-EN), Wright-Patterson AFB, Ohio 45433		10. PROGRAM ELEMENT, PROJECT, TASK AREA & WORK UNIT NUMBERS
11. CONTROLLING OFFICE NAME AND ADDRESS: Flight Essential Avionics Branch, Aeronautical Systems Division, Wright-Patterson AFB, Ohio 45433		12. REPORT DATE: June, 1978 13. NUMBER OF PAGES: 96
14. MONITORING AGENCY NAME & ADDRESS*(if different from Controlling Office)*		15. SECURITY CLASS. *(of this report)*: Unclassified 15a. DECLASSIFICATION/DOWNGRADING SCHEDULE

16. DISTRIBUTION STATEMENT *(of this Report)*

Approved for public release; distribution unlimited

17. DISTRIBUTION STATEMENT *(of the abstract entered in Block 20, if different from Report)*

18. SUPPLEMENTARY NOTES

Approved for public release; IAW AFR 190-17

JERRAL F. GUESS, Captain, USAF
Director of Information

19. KEY WORDS *(Continue on reverse side if necessary and identify by block number)*

Identification Friend or Foe (IFF)
Interrogator receiver
Probability of error
Probability of false alarm

20. ABSTRACT *(Continue on reverse side if necessary and identify by block number)*

The performance of a typical IFF interrogator receiver was evaluated against various types of received signals. The received signals that were considered represent environments of intentional as well as unintentional interference. The performance of the receiver was determined by studying the effects of an envelope detected version of the received signal on the decoder circuit in the interrogator. Probabilities of error and false alarm were approximated using a computer simulation for decoder operation.

DD FORM 1 JAN 73 1473 EDITION OF 1 NOV 65 IS OBSOLETE

SECURITY CLASSIFICATION OF THIS PAGE *(When Data Entered)*

Results indicated that many types of deterministic pulse formats will cause the decoder to respond at its maximum decode rate. Also, the simulated decoder would, under certain conditions, recognize pulses that did not specifically satisfy the pulse width requirement of the decoder. The decoder appears most vulnerable to noise-only signals whose bandwidths are greater than or equal to the overall bandwidth of the interrogator receiver. For these types of signals, as the power of the interference increases beyond a certain point, the performance of the decoder improves. For the signal-plus-noise case, results indicate that once the interference power reaches a certain value, increases in the power of the valid reply signal will not improve the performance of the decoder.